Published by
NIGERIAN SOCIETY OF PHYSICAL SCIENCES
Available online @ https://journal.nsps.org.ng/index.php/jnsps

J. Nig. Soc. Phys. Sci. 8 (2026) 3122

Journal of the Nigerian Society of Physical Sciences

Strategic interventions in schistosomiasis control: leveraging mass drug administration, public engagement, and intermediate host control to disrupt transmission dynamics

Agatha Abokwara*, Chinwendu E. Madubueze, Reuben I. Gweryina, Terhemen Aboiyar

Department of Mathematics, Joseph Sarwuan Tarka University, Makurdi, Benue State, Nigeria

Abstract

Schistosomiasis is caused by parasitic flatworms known as schistosomes. Humans become infected when they come into contact with freshwater containing these parasites. Many communities have only a limited understanding of how schistosomiasis spreads or how mass drug administration (MDA) can help to manage it. Furthermore, some regions neglect snail control efforts, despite snails are key intermediate hosts in disease transmission. In this study, we employ mathematical equations to illustrate how schistosomiasis spreads when public enlightenment campaigns, mass drug administration, and snail control measures are implemented. We calculate the control reproduction number, R_c, and examine the existence and stability of both the disease-free and endemic equilibrium states. Our results indicate that when people are aware of the disease, participate in mass drug administration, and intensify snail control efforts, the spread of the disease slows. Sensitivity analysis reveals that mass drug administration and increasing snail mortality rates are the most effective strategies for reducing R_c. Simulations suggest that improved sanitation and educating people about the benefits of taking medicine can reduce the number of infected individuals. Furthermore, treating water or introducing predatory fish can help to lower the population of disease-carrying snails. These findings provide valuable insights that can assist public health stakeholders in making informed decisions to control schistosomiasis.

DOI: 10.46481/jnsps.2026.3122

Keywords: Bifurcation, Control reproduction number, Stability analysis, Sensitivity analysis, Schistosomiasis

Article History :
Received: 10 September 2025
Received in revised form: 27 March 2026
Accepted for publication: 09 April 2026
Published: 14 May 2026

Communicated by: Pankaj Thakur

1. Introduction

Schistosomiasis is a disease affecting over 230 million people, with Nigeria being one of the most severely impacted countries [1, 2]. Women and children are at the greatest risk owing to their frequent visits to water bodies [3]. The *Schistosoma* parasite undergoes a complex metamorphosis, with mammals and freshwater snails serving as definitive and intermediate hosts, respectively [4]. Infected mammals excrete faeces or urine containing Schistosoma eggs, which hatch into miracidia. The miracidium penetrates a snail and develops into a cercaria until it encounters a mammal, penetrates its skin, and migrates to the liver of its host, where it matures into an adult [3, 5]. The progression of schistosomiasis infection occurs through distinct stages, including acute, chronic, and advanced phases [6]. At the advanced stage, *Schistosoma* worms develop complex mechanisms to modulate the host's immune system, thereby sustaining the infection [7]. Treatment alone does not eradicate the disease, as re-infection remains possible [8, 9].

*Corresponding author Tel.: +234-703-555-3966.
Email address: agathamicheal@gmail.com (Agatha Abokwara)

Mathematical modelling is an important tool in solving real-life challenges, as many researchers, such as Bada *et al.*, Chiyaka & Garira, Kadaleka *et al.*, Kanyi *et al.*, Koutou *et al.*, Lopez *et al.*, Nur *et al.*, Nur *et al.*, Ronoh *et al.*, and Tabo *et al.* [2, 10–18], have applied the concept of mathematical modelling to solve problems related to schistosomiasis. Among these researchers, Abokwara & Madubueze [19] examined the effect of public health education and snail control activities on the dynamics of schistosomiasis. Madubueze *et al.* [20] investigated the impact of public enlightenment campaigns, early diagnosis and treatment, and molluscicide use on the spread of the disease, while Temfack [21] tackled the implication of effective control using reaction-diffusion equations. Additionally, Wu *et al.* [22] explored the influence of seasonality and spatial heterogeneity, while Tabo *et al.* [23] considered biological control on the dynamics of schistosomiasis. Although these works have helped mitigate the challenges posed by schistosomiasis, they also have limitations, such as the impact of mass drug administration and environmental control activities on the elimination of snails in endemic communities. Mass drug administration (MDA) helps to mitigate disease morbidity or eliminate transmission [24], yet establishing effective control mechanisms remains challenging due to continued exposure of affected individuals to infested waters [25]. King and Bertsch [26] observed that schistosomiasis transmission could be reduced if MDA is combined with snail control activities in endemic communities, thereby mitigating infection and re-infection. Similarly, Abokwara & Madubueze [19] suggested that raising widespread awareness of schistosomiasis within communities would minimize the number of infected individuals in the population, while Madubueze *et al.* [20] argued that lowering the snail population would directly curb schistosomiasis transmission among humans, ultimately contributing to its eradication. Thus, this research develops an eight-compartment model incorporating suggestions from Abokwara & Madubueze, King & Bertsch and Madubueze *et al.* [19, 26, 27] in examining the influence of public enlightenment campaigns and environmental control activities for the elimination of snails in the surroundings while incorporating a compartment for individuals participating in MDA.

The remainder of the paper is organised as follows: Section 2 presents the model formulation. In Section 3, we examine the model's behaviour, including its equilibrium states, the control reproduction number, and the local and global stability of these states. Section 4 presents numerical simulations and a sensitivity analysis of the basic reproduction number to assess the influence of model parameters on disease dynamics. Finally, in Section 5, we present the results and draw conclusions.

2. Model formulation

The model examines the transformation of the *Schistosoma* parasite between mammals and snails at time t. The human population, N_h, is classified into four mutually exclusive compartments: susceptible humans, S_h; individuals involved in MDA, M_h; exposed (pre-infectious) humans, E_h; and infected humans, I_h. The snail population, N_s, is classified into susceptible snails, S_s, and infected snails, I_s. In addition, the miracidia population, M, and the cercariae population, C, representing the immature and mature developmental stages of the *Schistosoma* parasite, are considered. The susceptible human population, S_h, comprising individuals without infection, is recruited at a rate Λ_h, as well as through recovery from the infected stage of the disease at a rate η. Humans exit the susceptible class either as a result of infection, when they come into contact with cercariae at a rate λ_h; through natural death at a rate μ_h; or when they are introduced to MDA at a rate θ.

This is given by

$$\frac{dS_h}{dt} = \Lambda_h - \frac{(1-\omega)\beta_h C}{1+\varepsilon C} S_h - \eta I_h - \theta S_h - \mu_h S_h, \tag{1}$$

where β_h is the effective contact rate between susceptible humans and cercariae, ω is the public enlightenment rate, and ε is the limitation of the growth velocity of the pathogen [10].

The exposed human population, E_h, consists of individuals who have been exposed to contaminated water. The increase in this class arises from contact between susceptible humans and cercariae, at a rate given by $\frac{(1-\omega)\beta_h C}{1+\varepsilon C}$. Individuals exit this class at time t either through natural death at a rate μ_h, by progressing into the infectious stage of the disease at a rate α, or by moving into the MDA class following the administration of drugs at a rate θ. This yields

$$\frac{dE_h}{dt} = \frac{(1-\omega)\beta_h C S_h}{1+\varepsilon C} - \alpha E_h - \theta E_h - \mu_h E_h. \tag{2}$$

The infected human population, I_h, arises from the continuous deposition of parasite eggs, which become trapped in the host's tissues. Individuals are recruited into this class from the exposed compartment, E_h, at a rate α. They exit the class either through natural death at a rate μ_h, death resulting from the disease at a rate δ_h, or by moving into the MDA class following drug administration at a rate θ.

Since recovery from the disease is possible, individuals may return to the susceptible class at a rate η, yielding

$$\frac{dI_h}{dt} = \alpha E_h - \eta I_h - \theta I_h - \delta_h I_h - \mu_h I_h. \tag{3}$$

Due to the complex nature of the disease dynamics, mass drug administration (MDA) may be implemented in endemic environments. These MDA activities occur across all human classes at a rate θ, thereby reducing the spread of the disease within the environment. Individuals in this class exit through natural death at a rate μ_h. The dynamics is given by

$$\frac{dM_h}{dt} = \theta S_h + \theta E_h + \theta I_h - \mu_h M_h. \tag{4}$$

Infected humans shed a portion of the parasite eggs through their faeces or urine at a rate γ_h. These eggs enter the freshwater supply and hatch into free-swimming, ciliated larvae known as miracidia. The miracidia, M, die naturally at a rate μ_m. The rate of change is

$$\frac{dM}{dt} = \gamma_h I_h - \mu_m M. \tag{5}$$

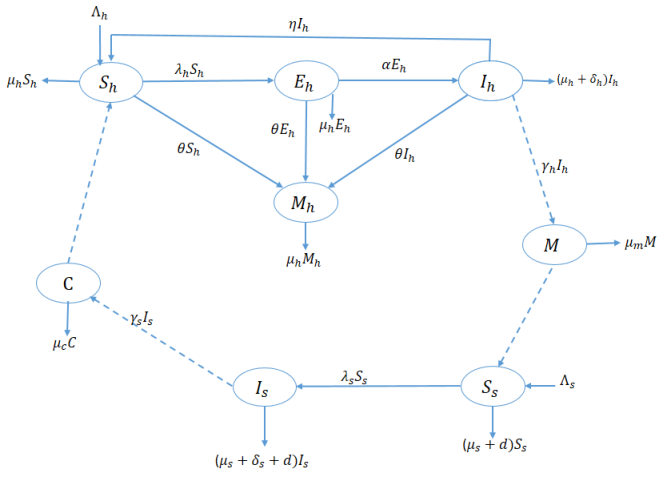

Figure 1: Schematic diagram of the schistosomiasis model with $\lambda_h = \frac{(1-\omega)\beta_h C}{1+\varepsilon C}$ and $\lambda_s = \frac{\beta_s M}{1+\varepsilon M}$.

The snail population is subdivided into susceptible snails, S_s and infected snails, I_s, at any time t. Recruitment into the susceptible snail class occurs through birth, while exit takes place as a result of disease infection when susceptible snails come into contact with miracidia at a rate $\frac{\beta_s M}{1+\varepsilon M}$; through death caused by environmental modification for snail control, at a rate d; or through natural death at a rate μ_s. The rate of change of this compartment is

$$\frac{dS_s}{dt} = \Lambda_s - \frac{\beta_s M}{1+\varepsilon M} S_s - \mu_s S_s - d S_s, \tag{6}$$

where β_s is the effective contact rate between miracidium and snail, and ε is the limitation of the growth velocity of the pathogen [10].

Snails get in contact with this contaminated water and become infected. These infected snails increase as a result of contact with miracidia at the rate, $\frac{\beta_s M}{1+\varepsilon M}$. They die either naturally at the rate, μ_s, or die as a result of the disease [28] at the rate, δ_s or as a result of environmental modification for snail control d. This yields

$$\frac{dI_s}{dt} = \frac{\beta_s M S_s}{1+\varepsilon M} - \delta_s I_s - d I_s - \mu_s I_s. \tag{7}$$

The infected snails release a free-living larva called cercariae at the rate γ_s, which is the shedding rate, and the free-living larva has the capacity of human infection. The cercariae die naturally at the rate μ_c.

$$\frac{dC}{dt} = \gamma_s I_s - \mu_c C. \tag{8}$$

The definitions of the parameters used in the schistosomiasis model, along with the model flow diagram, are provided in Table 1 and Figure 1, respectively. Figure 1 and Table 1 illustrate that the schistosomiasis model is represented by a set of non-linear ordinary differential equations, as described in System (9), with the initial conditions $S_h(0), M_h(0), S_s(0), E_h(0), I_h(0), M(0), I_s(0), C(0) > 0$.

$$\begin{aligned}
\frac{dS_h}{dt} &= \Lambda_h - (1-\omega)\frac{\beta_h C S_h}{1+\varepsilon C} + \eta I_h - \theta S_h - \mu_h S_h,\\
\frac{dE_h}{dt} &= (1-\omega)\frac{\beta_h C S_h}{1+\varepsilon C} - \theta E_h - \alpha E_h - \mu_h E_h,\\
\frac{dI_h}{dt} &= \alpha E_h - \eta I_h - \theta I_h - \mu_h I_h - \delta_h I_h,\\
\frac{dM_h}{dt} &= \theta S_h + \theta E_h + \theta I_h - \mu_h M_h,\\
\frac{dM}{dt} &= \gamma_h I_h - \mu_m M,\\
\frac{dS_s}{dt} &= \Lambda_s - \frac{\beta_s M S_s}{1+\varepsilon M} - \mu_s S_s - d S_s,\\
\frac{dI_s}{dt} &= \frac{\beta_s M S_s}{1+\varepsilon M} - \mu_s I_s - \delta_s I_s - d I_s,\\
\frac{dC}{dt} &= \gamma_s I_s - \mu_c C.
\end{aligned} \tag{9}$$

3. Qualitative analysis of the model

3.1. Positivity of the state variables

To show the positivity of the solution, we state and prove the following theorem.

Theorem 1. *The solutions $(S_h, E_h, I_h, M_h, M, S_s, I_s, C)$, of the system (9) are non-negative for all time $t > 0$ for any given non-negative initial conditions.*

Proof. We prove that the solution, S_h, is non-negative. Suppose that at time t_1, $S_h'(t_1) < 0$, $E_h(t_1) > 0$, $I_h(t_1) > 0$, $M_h(t_1) > 0$, $M(t_1) > 0$, $S_s(t_1) > 0$, $I_s(t_1) > 0$, $C(t_1) > 0$. From the first equation of system (9),

$$\begin{aligned}
S_h'(t_1) = \Lambda_h + \eta I_h(t_1) - \frac{(1-\omega)\beta_h C}{1+\varepsilon C}(t_1) S_h(t_1) - \theta S_h(t_1) - \mu_h S_h(t_1)\\
= \Lambda_h + \eta I_h(t_1) > 0,
\end{aligned}$$

contradicting the assumption that $S_h'(t_1) < 0$. Therefore, $S_h > 0$ for $t > 0$.

For E_h, assume there exists a time, t_2, $t_1 \neq t_2$ such that $E_h(t_2) = 0$, with $E_h'(t_2) < 0$ and all other variables being non-negative at $t \neq t_2$, then from the second equation of model (9),

$$\begin{aligned}
E_h'(t_2) &= \frac{(1-\omega)\beta_h C}{1+\varepsilon C}(t_2) S_h(t_2) - (\theta + \alpha + \mu) E_h(t_2)\\
&= \frac{(1-\omega)\beta_h C}{1+\varepsilon C}(t_2) S_h(t_2) > 0.
\end{aligned}$$

This is a contradiction since $E_h'(t_2) < 0$. Hence, $E_h \geq 0$ for $t > 0$.

For I_h, assume there exist a time, t_2 such that $I_h(t_3) = 0$, with $I_h'(t_3) < 0$ with all other variables being non negative at $t = t_3$, then from the third equation of model (9),

$$\begin{aligned}
I_h'(t_3) = \alpha E_h(t_3) - (\eta + \theta + \mu + \delta) I_h(t_3)\\
= \alpha E_h(t_3) > 0.
\end{aligned}$$

This is a contradiction since $I_h'(t_3) < 0$. Hence, $I_h \geq 0$ for $t > 0$.

Table 1: Parameter values used in the simulations.

Parameter	Symbol	Unit	Values	Sources
Recruitment rate for snail population	Λ_s	snails per time	20000	Assumed
Environmental modification for snail control	d	dimensionless	[0, 1]	Varied
Natural death rate for human population	μ_h	per time	$\frac{1}{365\times54}$	Calculated
Natural death rate for snail population	μ_s	per time	$\frac{50685}{10000000}$	[29]
Effective contact rate between miracidia and snail	β_s	per time	$\frac{615}{1000}$	[10]
Effective contact rate between cercariae and human	β_h	per time	$\frac{406}{1000}$	[10]
Movement rate of humans to the MDA class	θ	dimensionless	[0, 1]	Varied
Progression rate from exposed human class to infected human class	α	per time	$\frac{1}{55}$	[17]
Recovery rate of the infected human population	η	per time	$\frac{1}{43}$	[17]
Shedding rate of the infested snail population	γ_s	dimensionless	$\frac{26}{10}$	[28]
Shedding rate of the infested human population	γ_h	per time	$\frac{232}{10000}$	[28]
Mortality rate for the cercariae population	μ_c	humans per time	$\frac{4375}{10000}$	Calculated
Mortality rate for the miracidia population	μ_m	humans per time	$\frac{2778}{10000}$	Calculated
Public enlightenment campaigns	ω	dimensionless	[0, 1]	Varied
Disease-induced death rate for the infected human population	δ_h	per time	$\frac{27}{10000000}$	[30]
Disease-induced death rate for the snail population	δ_s	dimensionless	$\frac{4012}{10000000}$	[28]
Growth velocity limitation of the pathogen	ε	dimensionless	$\frac{2}{10}$	[10]

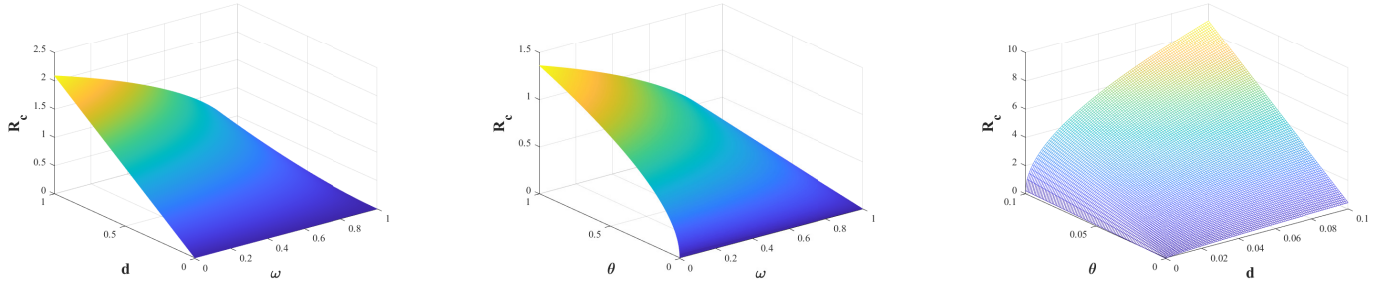

(a) (b) (c)

Figure 2: Surface plots showing the influence of (a) mass drug administration and snail control efforts, (b) public awareness and mass drug administration, and (c) snail control efforts and mass drug administration.

In the same way, it can be shown for M_h, M, S_s, I_s and C for $t > 0$. Therefore, we can conclude that the solutions $(S_h, E_h, I_h, M_h, M, S_s, I_s, C)$ of system (9) are non- negative for $t > 0$. This implies that the model is well-posed and makes biological sense, as living organisms cannot have negative sub-populations. □

It follows that the model is realistic and could help plan interventions.

3.2. Invariant region

For time $t \geqslant 0$, the model parameters make biological sense, that is, they are assumed to be non-negative with non-negative initial conditions. The model (9) will therefore be analysed in a suitable feasible region, obtained as follows. The total human population, N_h, at any time t, is given by

$$N_h = S_h + E_h + I_h + M_h, \tag{10}$$

M is the miracidia population, C is the cercariae population and N_s represents the total snail population given by

$$N_s = S_s + I_s, \tag{11}$$

with initial conditions $M(0) = M_0, C(0) = C_0, N_h(0) = N_{h0}$, and $N_s(0) = N_{s0}$ respectively. We state the following lemma.

Lemma 1. *All feasible solutions are uniformly bounded in a proper subset*

$$\varrho = \varrho_h \times \varrho_m \times \varrho_s \times \varrho_c,$$

where

$$\varrho = \left\{(S_h, E_h, I_h, M_h) \in \mathbb{R}^4_+ : N_h(t) \leq \frac{\Lambda_h}{\mu_h}\right\},$$

$$\varrho_m = \left\{M \in \mathbb{R}_+ : 0 < M(t) \leq \frac{\Lambda_h \gamma_h}{\mu_h \mu_m}\right\},$$

$$\varrho_s = \left\{(S_s, I_s) \in \mathbb{R}^2_+ : N_s(t) \leq \frac{\Lambda_s}{\mu_s + d}\right\},$$

and

$$\varrho_c = \{C \in \mathbb{R}_+ : 0 < C(t) \leq \frac{\Lambda_s \gamma_s}{(\mu_s + d)\mu_c}\}.$$

are subsets for human, miracidia, snail and cercariae populations, respectively.

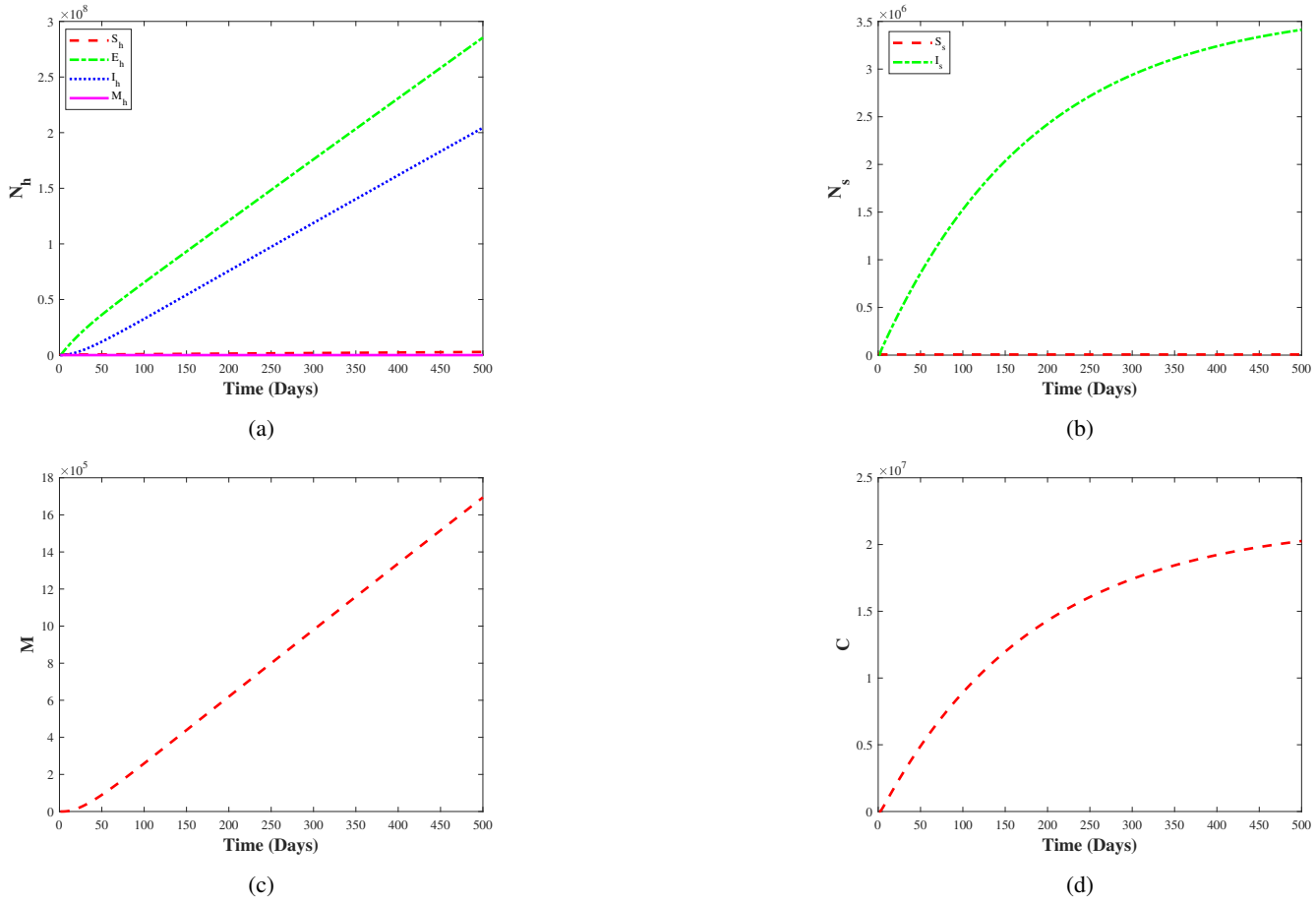

Figure 3: Baseline plots for (a) the human populations, (b) the snail populations, (c) the miracidia population, and (d) the cercaria population.

Proof. Considering the human population,

$$\frac{dN_h}{dt} = \Lambda_h - \mu_h N_h - \delta_h I_h < \Lambda_h - \mu_h N_h. \tag{12}$$

Applying Birkhoff and Rota theorem, Ref. [31] on differential inequality and integrating both sides of equation (12), we have

$$\int \frac{dN_h}{\Lambda_h - \mu_h N_h} \leq \int dt.$$

This implies that

$$\Lambda_h - \mu_h N_h \geq W_h \exp(-\mu_h t) \tag{13}$$

with W_h as a positive constant.

Furthermore, applying the initial conditions to equation (13), we obtain

$$\Lambda_h - \mu_h N_h \geq [\Lambda_h - \mu_h N_h(0)]\, e^{-\mu_h t},$$

which simplifies to

$$N_h \leq \frac{\Lambda_h}{\mu_h} - \{\frac{(\Lambda_h - \mu_h N_h(0))}{\mu_h}\} e^{-\mu_h t}. \tag{14}$$

As $t \longrightarrow \infty$ in equation (14), the human population size, N_h approaches $\frac{\Lambda_h}{\mu_h}$.

Therefore, all feasible regions of the human populations, S_h, E_h, I_h, and M_h enter the region

$$\varrho_h = \{(S_h, E_h, I_h, M_h) \in \mathbb{R}^4_+ : N_h \leq \frac{\Lambda_h}{\mu_h}\}.$$

For the miracidia population, we have from the fifth equation in system (9) that

$$\frac{dM}{dt} = \gamma_h I_h - \mu_m M.$$

But, $I_h \leq N_h$ and $I_h \leq N_h \leq \frac{\Lambda_h}{\mu_h}$.

Thus, we have

$$\frac{dM}{dt} \leq \frac{\gamma_h \Lambda_h}{\mu_h} - \mu_m M. \tag{15}$$

Applying Birkhoff & Rota theorem, Ref. [31] on differential inequality and integrating both sides of equation (15), we have

$$\int \frac{dM}{\gamma_h \frac{\Lambda_h}{\mu_h} - \mu_m M} \leq \int dt,$$

which implies that

$$-\frac{1}{\mu_m} \ln\left(\frac{\gamma_h \Lambda_h}{\mu_h} - \mu_m M\right) \leq t + V_m, \tag{16}$$

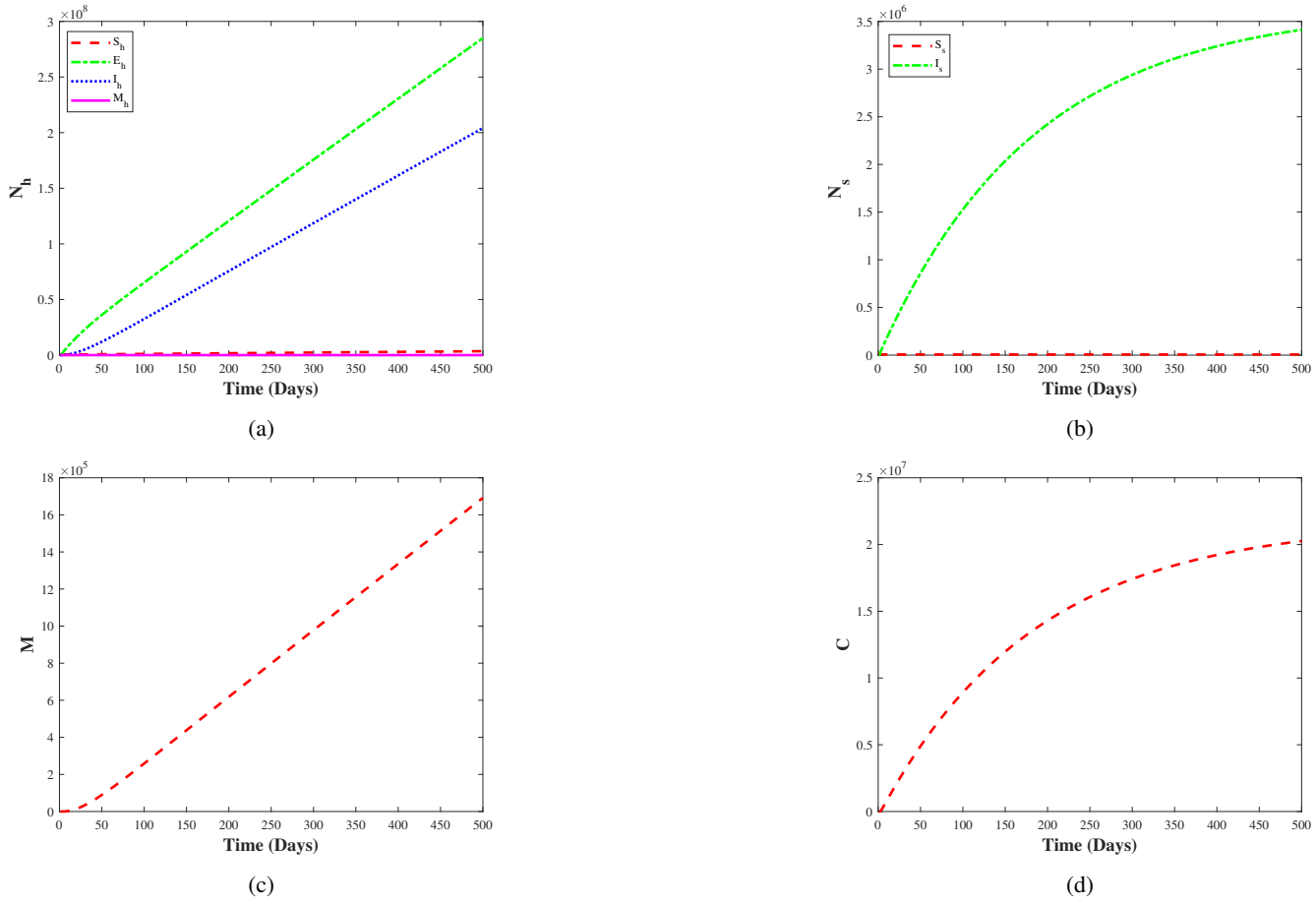

Figure 4: Plots for (a) the human populations, (b) the snail populations, (c) the miracidia population, and (d) the cercaria population. ($\omega = 0.2, \theta = d = 0$) .

with V_m as the constant of integration.

It follows from equation (16) that

$$\ln\left(\frac{\gamma_h\Lambda_h}{\mu_h} - \mu_m M\right) \geq -\mu_m(t + V_m).$$

Therefore,

$$\frac{\gamma_h\Lambda_h}{\mu_h} - \mu_m M \geq W_m e^{-\mu_m t}, \tag{17}$$

where W_m is a positive constant.

Furthermore, applying the initial condition, $M(0) = M_0$, to equation (17) yields

$$W_m \leq \frac{\gamma_h\Lambda_h}{\mu_h} - \mu_m M(0). \tag{18}$$

Substituting equation (18) into equation (17) gives

$$M \leq \frac{\Lambda_h\gamma_h}{\mu_h\mu_m} - \left[\frac{\gamma_h\Lambda_h}{\mu_h\mu_m} - \frac{\mu_m M(0)}{\mu_h}\right] e^{-\mu_m t}. \tag{19}$$

As $t \longrightarrow \infty$ in equation (19), the population size, M, approaches

$$M \leq \frac{\Lambda_h\gamma_h}{\mu_h\mu_m}.$$

Hence, the miracidia population will enter the positive invariant region, ϱ_m, where

$$\varrho_m = \{M \in \mathbb{R}_+ : 0 < M \leq \frac{\Lambda_h\gamma_h}{\mu_h\mu_m}\}.$$

For the snail population, we have

$$\frac{dN_s}{dt} = \Lambda_s - (\mu_s + d)N_s - \delta_s I_s < \Lambda_s - (\mu_s + d)N_s. \tag{20}$$

Applying Birkhoff & Rota theorem, Ref. [31] on differential inequality and integrating both sides of equation (20), we have

$$\Lambda_s - (\mu_s + d)N_s \geq W_s e^{-(\mu_s+d)t} \tag{21}$$

with W_s as a positive constant.

Applying the initial conditions $N_s(0) = N_{s0}$, to equation (21), we obtain

$$\Lambda_s - \mu_s N_s \geq [\Lambda_s - (\mu_s + d)N_s(0)]e^{-\mu_s t},$$

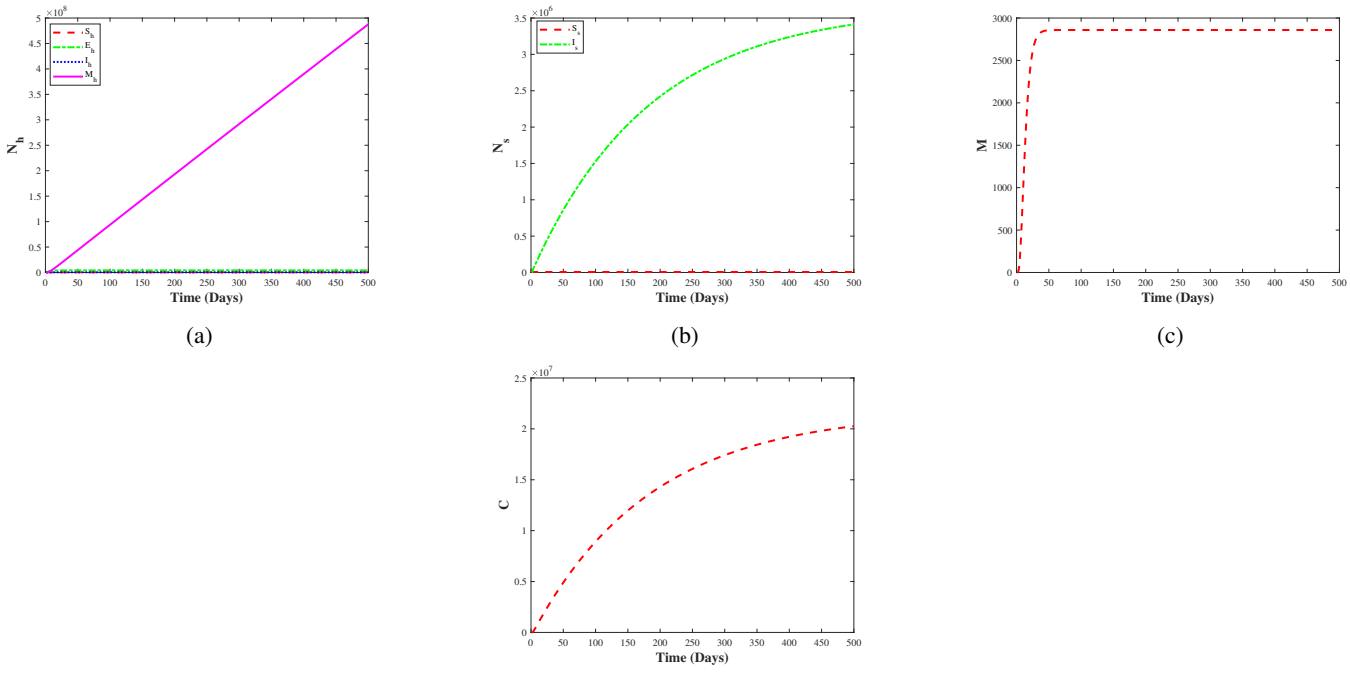

Figure 5: Plots of (a) the human populations, (b) the snail populations, (c) the miracidia population, and (d) the cercaria population. ($\theta = 0.2, \omega = d = 0$).

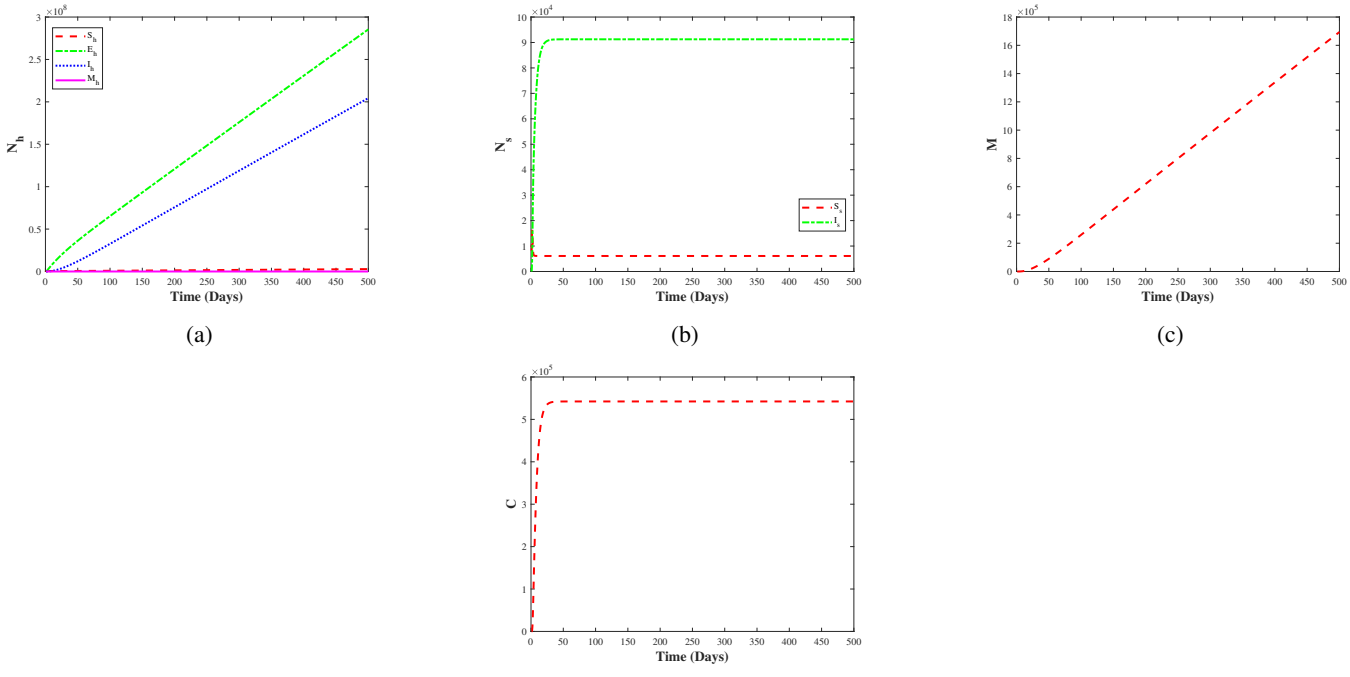

Figure 6: Plots of (a) the human populations, (b) the snail populations, (c) the miracidia population, and (d) the cercaria population. ($d = 0.2, \omega = \theta = 0$)

implying that □

$$N_s \leq \frac{\Lambda_s}{\mu_s} - \left[\frac{\Lambda_s - (\mu_s + d)N_s(0)}{\mu_s + d}\right]e^{-(\mu_s+d)t}. \quad (22)$$

As $t \longrightarrow \infty$ in equation (22), the snail population size, N_s approaches $\frac{\Lambda_s}{\mu_s}$.

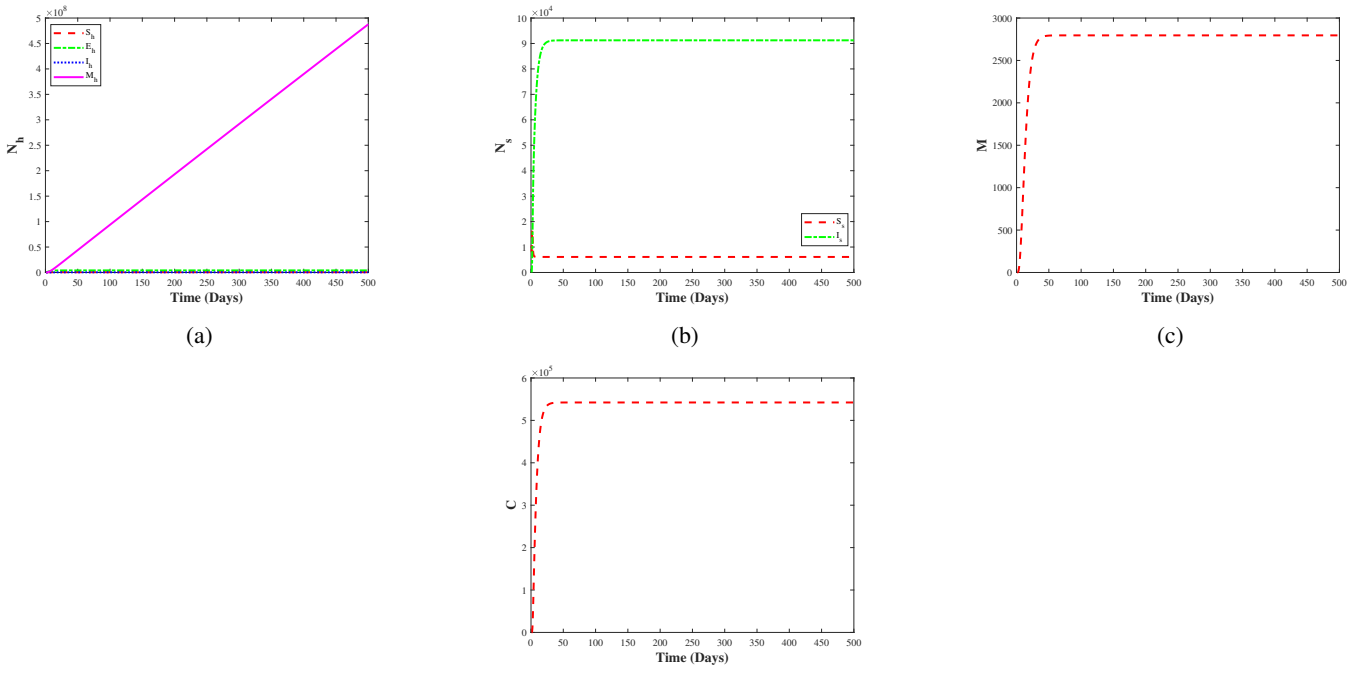

Figure 7: Plots of (a) the human populations, (b) the snail populations, (c) the miracidia population, and (d) the cercaria population. ($\omega = \theta = d = 0.2$)

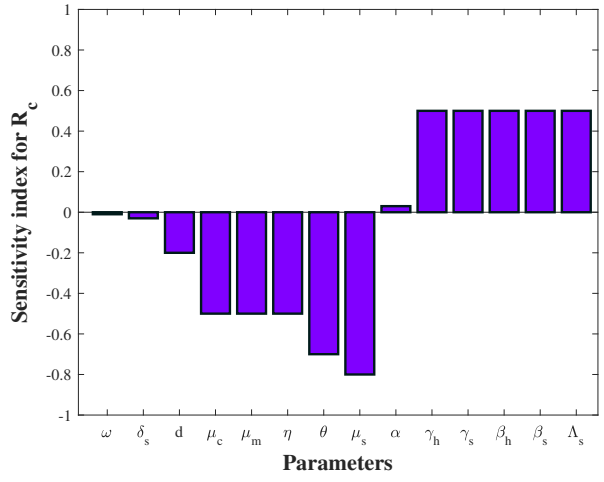

Figure 8: Normalised forward sensitivity indices of model parameters on the control reproduction number, R_c. ($\omega = 0.02,\ \theta = d = 0.001$).

Therefore, all feasible regions of the snail populations, S_s and I_s, enter the region

$$\varrho_s = \left\{(S_s, I_s) \in \mathbb{R}^2_+ : N_s(t) \leq \frac{\Lambda_s}{\mu_s + d}\right\}.$$

Furthermore, we have for cercariae population that

$$\frac{dC}{dt} = \gamma_s I_s - \mu_c C. \tag{23}$$

But, $I_s \leq N_s(t) \leq \frac{\Lambda_s}{\mu_s + d}$,

then

$$\frac{dC}{dt} \leq \frac{\gamma_s \Lambda_s}{\mu_s + d} - \mu_c C. \tag{24}$$

Applying Birkhoff & Rota theorem, Ref. [31] on differential inequality and integrating both sides of equation (24) gives

$$\frac{-1}{\mu_c} \ln\left[\frac{\gamma_s \Lambda_s}{\mu_s + d} - \mu_c C\right] \leq t + V_c \tag{25}$$

with V_c as the constant of integration.
It follows from equation (25) that

$$\ln\left[\frac{\gamma_s \Lambda_s}{\mu_s + d} - \mu_c C\right] \geq -\mu_c (t + V_c),$$

which implies that

$$\frac{\gamma_s \Lambda_s}{\mu_s + d} - \mu_c C \geq W_c e^{-\mu_c t}, \tag{26}$$

where W_c is a positive constant.
Applying the initial conditions to equation (26) yields

$$W_c \leq \frac{\gamma_s \Lambda_s}{\mu_s + d} - \mu_c C(0). \tag{27}$$

Substitute equation (27) into equation (26) and simplifying gives

$$C \leq \frac{\Lambda_s \gamma_s}{(\mu_s + d)\mu_c} - \left[\frac{\gamma_s \Lambda_s}{(\mu_s + d)\mu_c} - \frac{\mu_c C(0)}{\mu_s + d}\right] e^{-\mu_c t}. \tag{28}$$

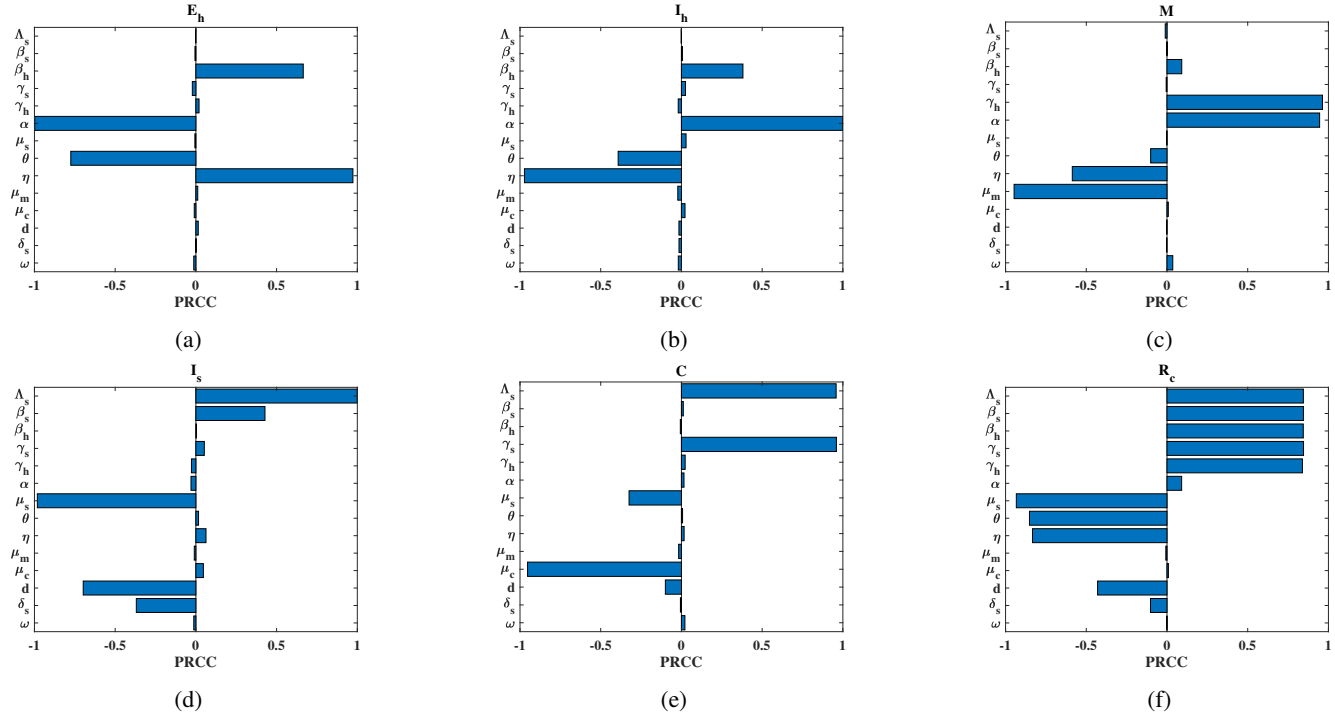

Figure 9: prcc results showing sensitivity indices of the model parameters with (a) the exposed human class, (b) the infected human class, (c) the miracidia population, (d) the infected snail population, (e) the cercariae population, and (f) the control reproduction number. ($\omega = 0.02,\ \theta = d = 0.001$).

As $t \longrightarrow \infty$ in equation (28), the population size, C, approaches $C \leq \frac{\Lambda_s \gamma_s}{(\mu_s + d)\mu_c}$.

Hence, the cercariae population will enter the positive invariant region

$$\varrho_c = \{C \in \mathbb{R}_+ : 0 < C \leq \frac{\Lambda_s \gamma_s}{(\mu_s + d)\mu_c}\}.$$

This implies that every solution with initial condition in $\mathbb{R}^8_+$ remains in that region for $t > 0$, which is a positively invariant set under the flow induced by the model, equation (9). Thus, the system, equation (9) is epidemiologically meaningful and mathematically well-posed in the interior of the domain, ϱ. Therefore, in this domain, it is sufficient to consider the dynamics of the flow generated by model equation (9).

It follows that the model system, equation (9) is biologically meaningful and mathematically valid, making it a reliable tool to slow down the spread of schistosomiasis.

3.3. The disease-free equilibrium state

An equilibrium state is one in which the system remains steady, with no changes recorded. This implies that the rate of change, given by $\frac{dX}{dt}$, is equal to zero. The disease-free equilibrium state implies that there is no infection, which means that

$$E_h = I_h = M = C = I_s = 0. \tag{29}$$

By the definition of an equilibrium state, it implies that

$$\begin{aligned}
\frac{dS_h}{dt} &= \Lambda_h - (1-\omega)\frac{\beta_h C S_h}{1+\varepsilon C} + \eta I_h - \theta S_h - \mu_h S_h = 0,\\
\frac{dE_h}{dt} &= (1-\omega)\frac{\beta_h C S_h}{1+\varepsilon C} - k_1 E_h = 0,\\
\frac{dI_h}{dt} &= \alpha E_h - k_2 I_h = 0,\\
\frac{dM_h}{dt} &= \theta S_h + \theta E_h + \theta I_h - \mu_h M_h = 0,\\
\frac{dM}{dt} &= \gamma_h I_h - \mu_m M = 0,\\
\frac{dS_s}{dt} &= \Lambda_s - \frac{\beta_s M S_s}{1+\varepsilon M} - \mu_s S_s - d S_s = 0,\\
\frac{dI_s}{dt} &= \frac{\beta_s M S_s}{1+\varepsilon M} - k_3 I_s = 0,\\
\frac{dC}{dt} &= \gamma_s I_s - \mu_c C = 0,
\end{aligned} \tag{30}$$

where

$$k_1 = \theta + \alpha + \mu_h,\ k_2 = \eta + \theta + \mu_h + \delta_h,\ k_3 = \mu_s + \delta_s + d. \tag{31}$$

Substituting equation (29) into system (30) gives the disease-free equilibrium state, $E^0 = (S_h^0, E_h^0, I_h^0, M_h^0, M^0, S_s^0, I_s^0, C^0)$.

$$E^0 = \left(\frac{\Lambda_h}{\mu_h + \theta}, 0, 0, \frac{\theta \Lambda_h}{\mu_h(\mu_h + \theta)}, 0, \frac{\Lambda_s}{\mu_s + d}, 0, 0\right). \tag{32}$$

3.3.1. The control reproduction number

The control reproduction number, R_c, represents the average number of new individuals to whom one infected per-

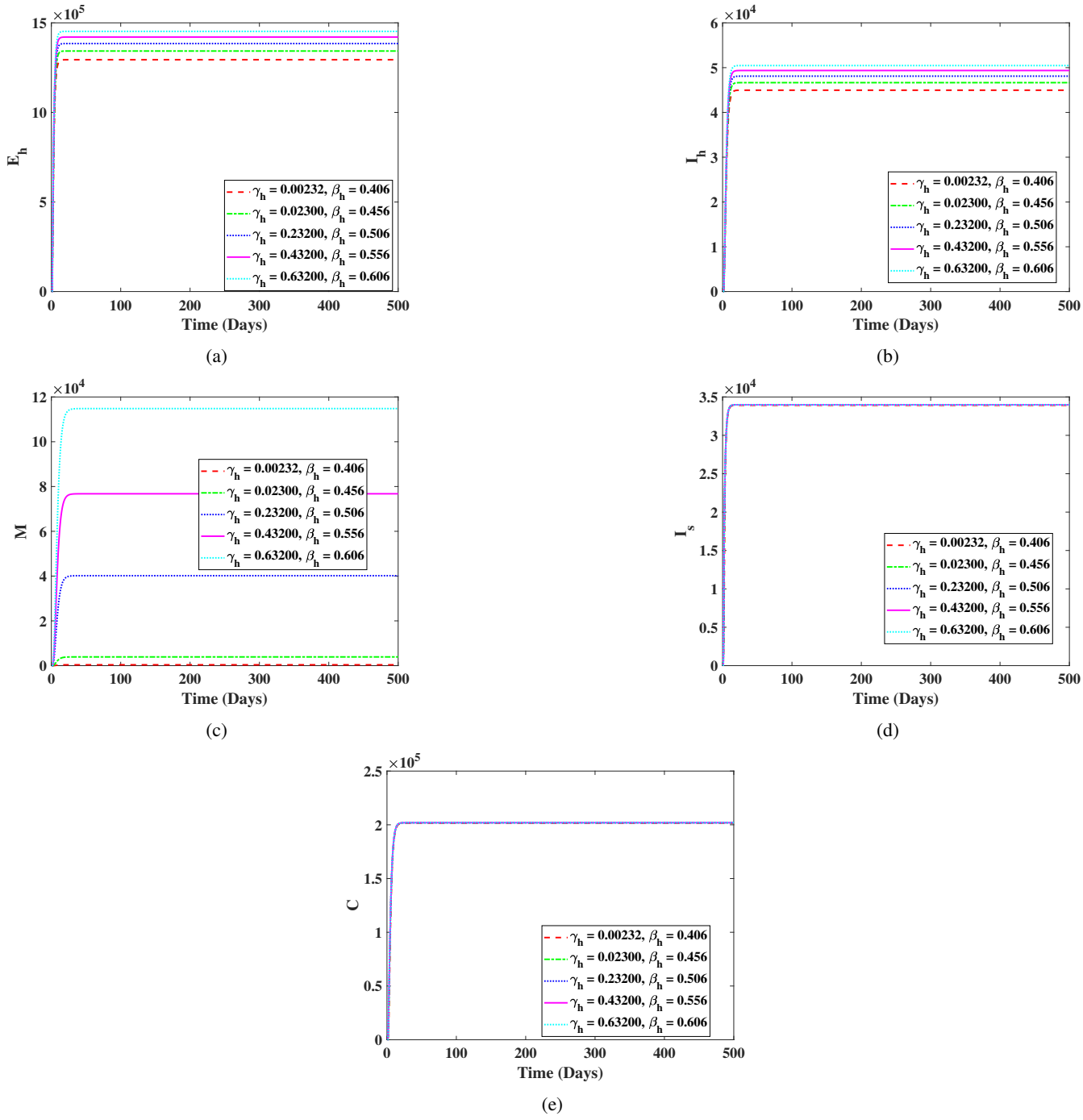

Figure 10: Numerical simulations of varying values of γ_h and β_h for (a) The Exposed human population E_h, (b) The Infected human population, (c) The miracidia population, (d) The infected snail population, and (e) The cercaria population. ($\omega = \theta = d = 50\%$) .

son can transmit schistosomiasis in a population where control measures are in place [32]. One way to calculate the control reproduction number, R_c, is by using the next-generation matrix approach, which involves finding the spectral radius while the system is at the disease-free equilibrium, E^0. The next-generation matrix is made up of two components; F and V, where $F = \frac{\partial F_i(E^0)}{\partial x_i}$ and $V = \frac{\partial V_i(E^0)}{\partial x_j}$. The F_i are the new infections while the V_i are transfers of infections from one compartment to another, and E_0 is the disease-free equilibrium state. R_c is the spectral radius of the matrix FV^{-1} with the associated matrix F and matrix V as Jacobian matrices of F_i and V_i at disease-free equilibrium state. The next-generation approach focuses on the compartments that involve individuals who are infected. We consider the infected compartments E_h, I_h, M, I_s and C. Applying the next-generation matrix method to the model (9)

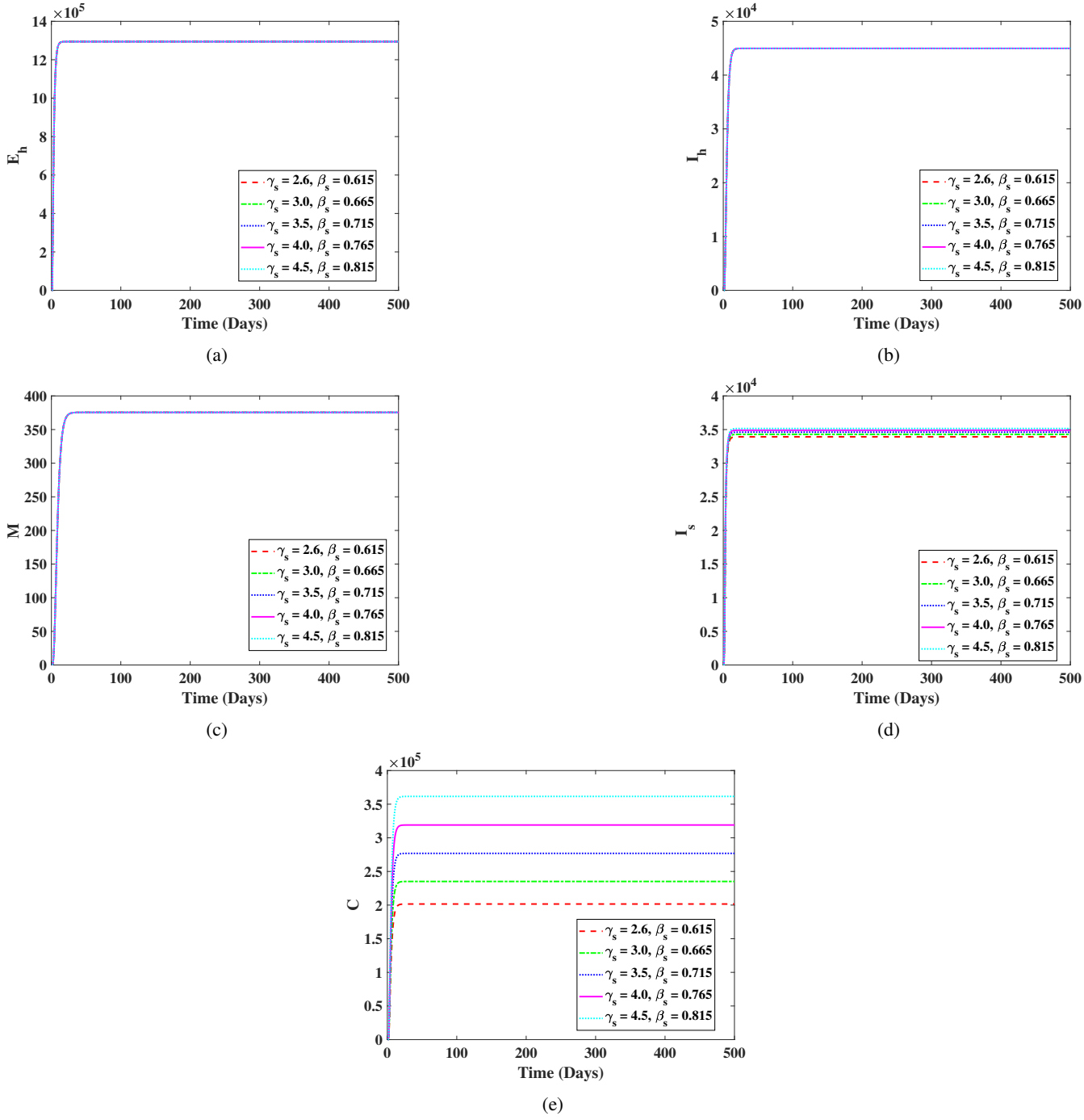

Figure 11: Numerical plots for varying values of γ_s and β_s for (a) The Exposed human population E_h, (b) The Infected human population I_h, (c) The miracidia population, (d) The infected snail population, I_s and (e) The cercaria population, C. ($\omega = \theta = d = 50\%$).

gives and

$$F = \begin{pmatrix} 0 & 0 & 0 & 0 & \frac{(1-\omega)\beta_h\Lambda_h}{\mu_h+\theta} \\ 0 & 0 & 0 & 0 & 0 \\ 0 & 0 & 0 & 0 & 0 \\ 0 & 0 & \frac{\beta_s\Lambda_s}{\mu_s+d} & 0 & 0 \\ 0 & 0 & 0 & 0 & 0 \end{pmatrix}, \quad V = \begin{pmatrix} k_1 & 0 & 0 & 0 & 0 \\ -\alpha & k_2 & 0 & 0 & 0 \\ 0 & -\gamma_h & \mu_m & 0 & 0 \\ 0 & 0 & 0 & k_3 & 0 \\ 0 & 0 & 0 & -\gamma_s & \mu_c \end{pmatrix}, FV^{-1} = \begin{pmatrix} 0 & 0 & 0 & \frac{(1-\omega)\beta_h\Lambda_h\gamma_s}{k_3\mu_c(\mu_h+\theta)} & \frac{(1-\omega)\beta_h\Lambda_h}{\mu_c(\mu_h+\theta)} \\ 0 & 0 & 0 & 0 & 0 \\ 0 & 0 & 0 & 0 & 0 \\ \frac{\beta_s\Lambda_s\gamma_h\alpha}{k_1k_2\mu_m(\mu_s+d)} & \frac{\beta_s\Lambda_s\gamma_h}{k_2\mu_m(\mu_s+d)} & \frac{\beta_s\Lambda_s}{\mu_m(\mu_s+d)} & 0 & 0 \\ 0 & 0 & 0 & 0 & 0 \end{pmatrix}.$$

The spectral radius of FV^{-1}, which is the control reproduc-

tion number is given by

$$R_c = \sqrt{\frac{(1-\omega)\Lambda_h\Lambda_s\beta_s\beta_h\gamma_h\gamma_s\alpha}{\mu_m\mu_c(\theta+\alpha+\mu_h)(\eta+\theta+\mu_h+\delta_h)(\mu_s+\delta_s+d)(\theta+\mu_h)(d+\mu_s)}} = \sqrt{R_{hm}R_{sc}}, \tag{33}$$

where

$$R_{hm} = \frac{(1-\omega)\Lambda_h\beta_h\gamma_h\alpha}{\mu_m(\theta+\alpha+\mu_h)(\eta+\theta+\mu_h+\delta_h)(\theta+\mu_h)}$$

and

$$R_{sc} = \frac{\Lambda_s\beta_s\gamma_s}{\mu_c(\mu_s+\delta_s+d)(d+\mu_s)}.$$

In this context, R_{sc} represents the impact of the snail population on the disease dynamics, while R_{hm} indicates the contribution of the human population. The basic reproduction number, R_c, is calculated as the geometric mean of R_{sc} and R_{hm}. This is because when an infected person enters a previously unexposed population, the parasite must first pass through a snail host before it can infect another human.

In the absence of mass drug administration, snail control activities and public enlightenment campaigns, we have the reproduction numbers as

$$\begin{aligned} R_{phe} &= \sqrt{\frac{\Lambda_h\Lambda_s\beta_s\beta_h\gamma_h\gamma_s\alpha}{\mu_m\mu_c(\theta+\alpha+\mu_h)(\eta+\theta+\mu_h+\delta_h)(\mu_s+\delta_s+d)(\theta+\mu_h)(d+\mu_s)}},\\ R_{mda} &= \sqrt{\frac{(1-\omega)\Lambda_h\Lambda_s\beta_s\beta_h\gamma_h\gamma_s\alpha}{\mu_m\mu_h\mu_c(\alpha+\mu_h)(\eta+\mu_h+\delta_h)(\mu_s+\delta_s+d)(d+\mu_s)}},\\ R_d &= \sqrt{\frac{(1-\omega)\Lambda_h\Lambda_s\beta_s\beta_h\gamma_h\gamma_s\alpha}{\mu_m\mu_s\mu_c(\theta+\alpha+\mu_h)(\eta+\theta+\mu_h+\delta_h)(\mu_s+\delta_s)(\theta+\mu_h)}}. \end{aligned} \tag{34}$$

In this case, R_{phe} denotes the disease spread without public enlightenment campaigns, R_{mda} denotes the spread without mass drug administration, and R_d denotes the spread without controlling the snails. For $\omega = \theta = d = 0$, we have the basic reproduction number as

$$R_0 = \sqrt{\frac{\Lambda_h\Lambda_s\beta_s\beta_h\gamma_h\gamma_s\alpha}{\mu_m\mu_c\mu_s\mu_h(\alpha+\mu_h)(\eta+\mu_h+\delta_h)(\mu_s+\delta_s)}}. \tag{35}$$

Comparing equation (33) and equation (35), $R_c \leq R_0$. This shows that each of the factors θ, ω, and d plays a role in how schistosomiasis spreads and behaves in the population. Thus,

$$\begin{aligned} &\lim_{\omega\longrightarrow 1} R_0 = 0,\\ &\lim_{\theta\longrightarrow 1} R_0 = \sqrt{\frac{(1-\omega)\Lambda_h\Lambda_s\beta_s\beta_h\gamma_h\gamma_s\alpha}{\mu_m\mu_c(1+\mu_h)(1+\alpha+\mu_h)(1+\eta+\mu_h+\delta_h)(\mu_s+\delta_s+d)(d+\mu_s)}},\\ &\lim_{d\longrightarrow 1} = \sqrt{\frac{(1-\omega)\Lambda_h\Lambda_s\beta_s\beta_h\gamma_h\gamma_s\alpha}{\mu_m\mu_c(1+\mu_s)(\theta+\alpha+\mu_h)(\eta+\theta+\mu_h+\delta_h)(\mu_s+\delta_s)(\theta+\mu_h)}}. \end{aligned} \tag{36}$$

Figure 2 shows the influence of public awareness, ω, mass drug administration, θ, and snail control efforts, d, on the control reproduction number. Parameter values used are from Table 1.

3.4. The endemic equilibrium state

The endemic equilibrium state, E^e, is the point at which schistosomiasis persists in both humans and snails. We find this point by setting the rate of change in the model, equation (9) over time to zero and solving for the values of the variables. Recall that

$$\lambda_h = \frac{(1-\omega)\beta_h C}{1+\varepsilon C} \text{ and } \lambda_s = \frac{\beta_s M}{1+\varepsilon M}.$$

We have at equilibrium state that

$$\begin{aligned} &E_h = \frac{\lambda_h S_h}{k_1},\ I_h = \frac{\alpha\lambda_h S_h}{k_1k_2},\ I_s = \frac{\lambda_s S_s}{k_3},\\ &C = \frac{\gamma_s I_s}{\mu_c},\ M = \frac{\gamma_h I_h}{\mu_m},\ M_h = \frac{\theta(S_h+E_h+I_h)}{\mu_m}. \end{aligned} \tag{37}$$

Substitute equation (37) into the first and sixth equations of system, equation (9) and simplify yields

$$S_h^e = \frac{\Lambda_k k_1 k_2}{ak_1k_2 + (k_1k_2 - \alpha\eta)\lambda_h},\ S_s^e = \frac{\Lambda_s}{e+\lambda_s}, \tag{38}$$

where $a = \theta + \mu_h$, $e = \mu_s + d$. Substituting equations (37) and (38) into $\lambda_s = \frac{\beta_s M}{1+\varepsilon M}$ yields

$$\lambda_s = \frac{\alpha\Lambda_h\beta_s\gamma_s\gamma_h}{\alpha\varepsilon\Lambda_h\gamma_h + b\mu_m)\lambda_h + \alpha k_1k_2\mu_m},$$

with $b = k_1k_2 - \alpha\eta > 0$. Substituting λ_s into equations (37) and (38), simplify and substitute the outcome into

$$\lambda_h = \frac{(1-\omega)\beta_h C}{1+\varepsilon C}$$

gives

$$\lambda_h = 0 \text{ or } \lambda_h = \frac{\alpha\Lambda_h\Lambda_h(1-\omega)\beta_h\beta_s\gamma_h\gamma_s - aek_1k_2k_3\mu_m\mu_c}{A},$$

where

$$A = \alpha\varepsilon\Lambda_h\Lambda_s\beta_s\gamma_h\gamma_s + \alpha\Lambda_h\beta_s\gamma_h k_3\mu_c - ek_3\mu_c(\alpha\varepsilon\Lambda_h\gamma_h + b\mu_m).$$

With the definition of R_c, we have

$$\lambda_h^e = \frac{B(R_c^2-1)}{A},$$

where $B = aek_1k_2k_3\mu_m\mu_c$. Substituting λ_h into λ_s yields

$$\lambda_s^e = \frac{\alpha\Lambda_h\beta_s\gamma_h B(R_c^2-1)}{Aak_1k_2\mu_m + B(\alpha\varepsilon\Lambda_h\gamma_h + b\mu_m)(R_c^2-1)}.$$

If you substitute $S_h^e = \frac{\Lambda_h k_1k_2}{ak_1k_2+b\lambda_h}$ and $S_s^e = \frac{\Lambda_s}{e+\lambda_s}$ into equation (37), it yields

$$\begin{aligned} &S_h^e = \frac{\Lambda_h k_1k_2}{ak_1k_2+b\lambda_h^e},\ E_h^e = \frac{\lambda_h^e\Lambda_h k_2}{ak_1k_2+b\lambda_h^e},\\ &I_h^e = \frac{\alpha\lambda_h^e\Lambda_h}{ak_1k_2+b\lambda_h^e},\ M_h^e = \frac{\theta\Lambda_h(\alpha\lambda_h^e + k_1k_2 + k_2\lambda_h^e)}{(ak_1k_2+b\lambda_h^e)\mu_h},\\ &S_s^e = \frac{\Lambda_s}{e+\lambda_s^e},\ I_s^e = \frac{\lambda_s^e\Lambda_s}{(e+\lambda_s^e)k_3},\\ &M^e = \frac{\gamma_h\alpha\lambda_h^e\Lambda_h}{(ak_1k_2+b\lambda_h^e)\mu_m},\ C^e = \frac{\gamma_s\lambda_s^e\Lambda_s}{(e+\lambda_s^e)k_3\mu_c}. \end{aligned} \tag{39}$$

3.5. Stability of the equilibrium states

3.5.1. Local stability of the disease-free equilibrium state

The local stability of the disease-free equilibrium (DFE) is determined by the control reproduction number, R_c, which is calculated using the next generation operator [32]. To assess this stability, we apply the method of linearization around the equilibrium point. We now present and prove the following theorem.

Theorem 2. *If E^0 is the DFE of the model, then E^0 is locally asymptotically stable if $R_c < 1$, but unstable if $R_c > 1$.*

Proof. The Jacobian matrix at DFE, E^0, is given by

$$J(E^0) = \begin{pmatrix} -(\theta+\mu_h) & 0 & \eta & 0 & 0 & 0 & 0 & -\frac{(1-\omega)\beta_h\Lambda_h}{\theta+\mu_h} \\ 0 & -k_1 & 0 & 0 & 0 & 0 & 0 & \frac{(1-\omega)\beta_h\Lambda_h}{\mu_h+\theta} \\ 0 & \alpha & -k_2 & 0 & 0 & 0 & 0 & 0 \\ \theta & \theta & \theta & -\mu_h & 0 & 0 & 0 & 0 \\ 0 & 0 & \gamma_h & 0 & -\mu_m & 0 & 0 & 0 \\ 0 & 0 & 0 & 0 & -\frac{\beta_s\Lambda_s}{\mu_s+d} & -(\mu_s+d) & 0 & 0 \\ 0 & 0 & 0 & 0 & \frac{\beta_s\Lambda_s}{\mu_s+d} & 0 & -k_3 & 0 \\ 0 & 0 & 0 & 0 & 0 & 0 & \gamma_s & -\mu_c \end{pmatrix}.$$

The eigenvalues of the Jacobian matrix $J(E^0)$ are $-(\theta+\mu_h)$, $-\mu_h$ and the roots of the characteristic equation

$$\lambda^6 + A_1\lambda^5 + A_2\lambda^4 + A_3\lambda^3 + A_4\lambda^2 + A_5\lambda + A_6 = 0, \tag{40}$$

where

$$\begin{aligned}
A_1 &= \mu_c + k_3 + \mu_s + d + \mu_m + k_2 + k_1,\\
A_2 &= d(k_1 + k_2 + k_3 + \mu_c + \mu_m) + k_1(k_2 + k_3 + \mu_c + \mu_m + \mu_s) + k_2(k_3 + \mu_c + \mu_m + \mu_s)\\
&\quad + \mu_c\mu_m + \mu_c\mu_s + \mu_s\mu_m,\\
A_3 &= k_1(dk_2 + k_3d + \mu_c d + d\mu_m + k_3k_2 + \mu_c k_2 + \mu_m k_2 + \mu_s k_2 + \mu_c k_3 + k_3\mu_m + k_3\mu_s + \mu_c\mu_m\\
&\quad + \mu_c\mu_s + \mu_s\mu_m) + k_2(k_3d + \mu_c d + d\mu_m + \mu_c k_3 + k_3\mu_m + k_3\mu_s + \mu_c\mu_m + \mu_c\mu_s + \mu_s\mu_m)\\
&\quad + k_3(\mu_c d + d\mu_m + \mu_c\mu_m + \mu_c\mu_s + \mu_s\mu_m) + d\mu_c\mu_m + \mu_c\mu_m\mu_s,\\
A_4 &= dk_1k_2k_3 + dk_1k_2\mu_c + dk_1k_2\mu_m + dk_1k_3\mu_c + dk_1k_3\mu_m + dk_1\mu_c\mu_m + dk_2k_3\mu_c + dk_2k_3\mu_m\\
&\quad + dk_2\mu_c\mu_m + dk_3\mu_c\mu_m + k_1k_2k_3\mu_c + k_1k_2k_3\mu_m + k_1k_2k_3\mu_s + k_1k_2\mu_c\mu_m + k_1k_2\mu_c\mu_s + k_1k_2\mu_m\mu_s\\
&\quad + k_1k_3\mu_c\mu_m + k_1k_3\mu_c\mu_s + k_1k_3\mu_m\mu_s + k_1\mu_c\mu_m\mu_s + k_2k_3\mu_c\mu_m + k_2k_3\mu_c\mu_s + k_2k_3\mu_m\mu_s\\
&\quad + k_2\mu_c\mu_m\mu_s + k_3\mu_c\mu_m\mu_s,\\
A_5 &= (\mu_s + d)\left(\frac{1}{\mu_m} + \frac{1}{\mu_c} + \frac{1}{k_1} + \frac{1}{k_2} + \frac{1}{k_3}\right) + (1 - R_c^2),\\
A_6 &= (d + \mu_s)(1 - R_c^2).
\end{aligned}$$

Here, $A_i > 0$, $i \in [1, 6]$ and the roots of the polynomial have real parts.

Thus, the stability of the disease-free equilibrium of the model (9) is determined solely by the sign of the constant term of the characteristic equation where all parameters are non-negative [33]. Also, $A_1, A_2, A_3, A_4, A_5, A_6$ has the property that $A_1, A_2, A_3, A_4, A_5, A_6 > 0$. Hence, we can conclude that the eigenvalues of the system have negative real parts if $R_c < 1$, therefore, the DFE, E^0, is locally asymptotically stable if $R_c < 1$. □

Schistosomiasis can be effectively controlled if detected early, highlighting the importance of proactive measures such as public enlightenment campaigns (ω). This also indicates that, under current circumstances namely, sustained interventions comprising MDA, public enlightenment campaigns, and snail control efforts when the control reproduction number, R_c, is maintained below unity, sporadic introductions of the parasite are insufficient to initiate endemic transmission. Under these conditions, the disease cannot propagate autonomously within the population. Nevertheless, regular monitoring and prompt responses remain essential, even when the situation appears to be under control.

3.5.2. Bifurcation analysis

We study how certain factors influence the spread of the disease by examining a critical point called bifurcation, where the reproduction number, $R_c = 1$. If a backward bifurcation happens, it means the schistosomiasis can persist in different steady states even when R_c is less than 1. This makes predicting and controlling the disease more complicated [34]. We investigate the bifurcation of the model at $R_c = 1$ using the centre manifold theorem by Castillo-Chavez & Song [35] with

$$p_1 = \sum_{k,i,j=1}^{n} m_k w_i w_j \frac{\partial^2 q_k(E^0)}{\partial x_i \partial x_j} \text{ and } p_2 = \sum_{k,i=1}^{n} m_k w_i \frac{\partial^2 q_k(E^0)}{\partial x_i \partial \pi}$$

as bifurcation coefficients and π as bifurcation parameter. Let $\beta_s = \hat{\beta}_s$ be the bifurcation parameter at $R_c^2 = 1 = R_c$ then

$$\hat{\beta}_s = \frac{k_1k_2k_3\mu_m\mu_c(\theta+\mu_h)(d+\mu_s)}{(1-\omega)\Lambda_h\Lambda_s\beta_h\gamma_h\gamma_s\alpha}.$$

Let

$$x_1 = S_h,\ x_2 = E_h,\ x_3 = I_h,\ x_4 = M_h,\ x_5 = M,\ x_6 = S_s,\ x_7 = I_s,\ x_8 = C, \tag{41}$$

and $q_1, q_2, q_3, q_4, q_5, q_6, q_7, q_8$ be the right hand sides of the system of equations (9). Therefore the non-zero second order partial derivatives of $q_1, q_2, q_3, q_4, q_5, q_6, q_7, q_8$ at disease-free equilibrium state, E_0 results in

$$\begin{aligned}
&\frac{\partial^2 q_1(E^0)}{\partial x_1\partial x_8} = \frac{\partial^2 q_1(E^0)}{\partial x_8\partial x_1} = -(1-\omega)\beta_h,\\
&\frac{\partial^2 q_2(E^0)}{\partial x_1\partial x_8} = \frac{\partial^2 q_2(E^0)}{\partial x_8\partial x_1} = (1-\omega)\beta_h,\\
&\frac{\partial^2 q_6(E^0)}{\partial x_5\partial x_6} = \frac{\partial^2 q_6(E^0)}{\partial x_6\partial x_5} = -\hat{\beta}_s,\ \frac{\partial^2 q_7(E^0)}{\partial x_5\partial x_6} = \frac{\partial^2 q_7(E^0)}{\partial x_6\partial x_5} = \hat{\beta}_s,
\end{aligned} \tag{42}$$

and

$$\frac{\partial^2 q_6(E^0)}{\partial x_5\partial\hat{\beta}_s} = -\frac{\Lambda_s}{\mu_s + d},\ \frac{\partial^2 q_7(E^0)}{\partial x_5\partial\hat{\beta}_s} = \frac{\Lambda_s}{\mu_s + d}. \tag{43}$$

Additionally, the left and right eigenvectors w and m are given as

$$\begin{aligned}
&m_1 = m_4 = m_6 = 0,\ m_8 = m_8 > 0.\\
&m_2 = \frac{\alpha\hat{\beta}_s\Lambda_s\gamma_s\gamma_h}{k_1k_2k_3\mu_m(\mu_s+d)}m_8,\ m_3 = \frac{\hat{\beta}_s\Lambda_s\gamma_h\gamma_s}{k_2k_3\mu_m(\mu_s+d)}m_8,\\
&m_5 = \frac{\hat{\beta}_s\Lambda_s\gamma_s}{(\mu_s+d)\mu_m k_3}m_8,\ m_7 = \frac{\gamma_s}{k_3}m_8,
\end{aligned} \tag{44}$$

and

$$
\begin{aligned}
w_1 &= -\frac{\beta_h\Lambda_h(1-\omega)}{\theta+\mu_h}\left[\frac{k_1k_2-\eta\alpha}{k_1k_2}\right]w_8, w_2 = \frac{\beta_h\Lambda_h(1-\omega)}{k_1(\mu_h+\theta)}w_8,\\
w_3 &= \frac{\beta_h\Lambda_h\alpha(1-\omega)}{k_1k_2(\theta+\mu_h)}w_8,\\
w_4 &= \frac{\theta\beta_h\Lambda_h(1-\omega)}{\mu_h(\mu_h+\theta)}\left[1-\frac{\eta\alpha}{k_1k_2}+\frac{1}{k_1}+\frac{\alpha}{k_1k_2}\right]w_8,\\
w_5 &= \frac{\gamma_h\beta_h\Lambda_h\alpha(1-\omega)}{k_1k_2\mu_m(\theta+\mu_h)}w_8,\ w_6 = -\frac{\hat{\beta}_s\Lambda_s\gamma_h\beta_h\Lambda_h\alpha(1-\omega)}{k_1k_2(\theta+\mu_h)(\mu_s+d)^2}w_8,\\
w_7 &= \frac{\hat{\beta}_s\Lambda_s\gamma_h\beta_h\alpha(1-\omega)}{k_1k_2k_3\mu_m(\mu_s+d)(\theta+\omega)}w_8,\ w_8 = w_8 > 0,
\end{aligned}
\tag{45}
$$

with $\mathbf{w}\cdot\mathbf{m} = 1$, where $\mathbf{w} = (w_1, w_2, w_3, w_4, w_5, w_6, w_7, w_8)$ and $\mathbf{m} = (m_1, m_2, m_3, m_4, m_5, m_6, m_7, m_8)$. Employing the non-zero second order partial derivatives of equation (42) and equation (43), we have

$$
\begin{aligned}
p_1 &= m_2w_1w_8\frac{\partial^2q_2(E^0)}{\partial x_1\partial x_8} + m_7w_5w_6\frac{\partial^2q_7(E^0)}{\partial x_5\partial x_6}\\
&\text{and}\\
p_2 &= m_7w_5\frac{\partial^2q_7(E^0)}{\partial x_5\partial\hat{\beta}_s}.
\end{aligned}
\tag{46}
$$

Substituting equations (44) and (45) into equation (46)

$$
\begin{aligned}
p_1 &= -m_8w_8^2\left[\frac{\beta_h\Lambda_h^2(1-\omega)^2\mu_c}{\hat{\beta}_s\gamma_s}\left(\frac{k_1k_2-\eta\alpha}{k_1k_2}\right)+\frac{\mu_c^2k_3\mu_m}{\Lambda_s}\right],\\
p_2 &= \frac{\Lambda_s\Lambda_h\gamma_h\gamma_s\beta_h\alpha m_8w_8(1-\omega)}{k_1k_2k_3\mu_m(\theta+\mu_h)(\mu_s+d)} > 0,
\end{aligned}
\tag{47}
$$

and $k_1k_2 - \alpha\eta > 0$. A forward bifurcation occurs since $p_1 < 0$ and $p_2 > 0$. Forward bifurcation implies that when $R_c < 1$, the disease-free equilibrium state, E^0, is stable, that is, the disease dies out. Epidemiologically, this means there is minimal risk of sustained transmission below this threshold. In comparison, when $R_c > 1$, the endemic equilibrium persists in the population. Furthermore, the endemic equilibrium, E^e becomes globally asymptotically stable when $R_c > 1$, while the disease-free equilibrium, E^0 is globally asymptotically stable when $R_c < 1$.

Thus, the World Health Organization [36] underscores the resilient nature of schistosomiasis, even under conditions where transmission potential is low due to environmental and behavioural factors. Colley *et al.* [37] further explain its persistence, highlighting the parasite's ability to remain in small endemic pockets. King [38] emphasises that patchy transmission can sustain the disease burden in endemic communities over extended periods.

3.5.3. Global stability of the disease-free equilibrium state

The following theorem establishes the global stability of the DFE, E^0.

Theorem 3. *The DFE, E^0 of system of equations (9) is globally asymptotically stable if $R_c \le 1$ and unstable if $R_c > 1$.*

Proof. Let us define the new variables and break the system given by equation (9) into subsystems. We use the notation $X_1 = (S_h, M_h, S_s)$, which denotes the number of susceptible individuals and individuals undergoing MDA. In addition, the notation $Y_1 = (E_h, I_h, M, I_s, C)$ denotes the numbers of exposed and infected individuals as well as the miracidia and cercariae compartments. The system can be presented as

$$
\begin{aligned}
\frac{dX_1}{dt} &= F(X_1, Y_1),\\
\frac{dY_1}{dt} &= G(X_1, Y_1), \text{where}\\
&X_1 \in \mathbb{R}^3_+, Y_1 \in \mathbb{R}^5_+.
\end{aligned}
$$

Then, the two vector-valued functions are

$$
\begin{aligned}
F(X_1, Y_1) = (&\Lambda_h - (1-\omega)\frac{\beta_hCS_h}{1+\varepsilon C} + \eta I_h - \theta S_h - \mu_hS_h,\\
&\theta S_h + \theta E_h + \theta I_h - \mu_hM_h,\\
&\Lambda_s - \frac{\beta_sMS_s}{1+\varepsilon M} - \mu_sS_s - dS_s)^T,
\end{aligned}
$$

$$
\begin{aligned}
G(X_1, Y_1) = (&(1-\omega)\frac{\beta_hCS_h}{1+\varepsilon C} - k_1E_h,\\
&\alpha E_h - k_2I_h,\\
&\gamma_hI_h - \mu_mM,\\
&\frac{\beta_sMS_s}{1+\varepsilon M} - k_3I_s,\\
&\gamma_sI_s - \mu_cC)^T,
\end{aligned}
$$

where T denotes the transpose. For simplicity, we identify X_1 with $(X_1, 0)$ and Y_1 with $(0, Y_1) \in \mathbb{R}^3_+ \times \mathbb{R}^5_+$. Hence the reduced system: $\frac{dX_1}{dt} = F(X_1, 0)$;

$$
\begin{aligned}
\frac{dS_h}{dt} &= \Lambda_h - \theta S_h - \mu_hS_h,\\
\frac{dM_h}{dt} &= \theta S_h - \mu_hM_h,\\
\frac{dS_s}{dt} &= \Lambda_s - \mu_sS_s - dS_s.
\end{aligned}
\tag{48}
$$

The Jacobian matrix of the subsystem (48) is given as

$$
J(x^*) = \begin{pmatrix} -(\theta+\mu_h) & 0 & 0\\ \theta & -\mu_h & 0\\ 0 & 0 & -(\mu_s+d)\end{pmatrix}
$$

with negative eigenvalues $-(\theta+\mu_h)$, $-\mu_h$, and $-(\mu_s+d)$, and $X^* = (S_h^{**}, M_h^{**}, S_s^{**}) = \left(\frac{\Lambda_h}{\mu_h+\theta}, \frac{\theta\Lambda_h}{\mu_h(\mu_h+\theta)}, \frac{\Lambda_s}{\mu_s+d}\right)$ is a global asymptotically stable equilibrium point for the reduced system $\frac{dX_1}{dt}F(X_1, 0)$. The asymptotic dynamics are independent of initial conditions in $\mathbb{R}^8_+$. According to Castillo-Chavez *et al.* [39], the fixed point X^* is a globally asymptotically stable equilibrium of system (9) provided that $R_c < 1$ is locally asymptotically stable and the assumptions $\frac{dX_1}{dt} = F(X_1, 0), X^0$ is globally asymptotically stable.

The second condition states that $G(X_1, Y_1) = AY - G^*(X_1, Y_1)$, where $G(X_1, Y_1) \ge 0$ for $X_1, Y_1 \in \varrho$, and $A = D_YG(X^*, 0)$ is an $M-matrix$.

Clearly $G(X_1, Y_1)$ satisfies the condition that

$G(X_1, 0) = 0$ and $G(X_1, Y_1) = A^*Y_1 - G^*(X_1, Y_1), G^*(X_1, Y_1) \geq 0$, where

$$A^* = D_Y G(X_1, 0) = \begin{pmatrix} -k_1 & 0 & 0 & 0 & \frac{(1-\omega)\beta_h\Lambda_h}{\theta+\mu_h} \\ \alpha & -k_2 & 0 & 0 & 0 \\ 0 & \gamma_h & -\mu_m & 0 & 0 \\ 0 & 0 & \frac{\beta_s\Lambda_s}{\mu_s+d} & -k_3 & 0 \\ 0 & 0 & 0 & \gamma_s & -\mu_c \end{pmatrix}$$

and

$$G^*(X_1, Y_1) = \begin{pmatrix} \beta_h C\left(\frac{\Lambda_h}{\mu_h+\theta} - S_h\right) \\ 0 \\ 0 \\ \beta_s M\left(\frac{\Lambda_s}{\mu_s+d} - S_s\right) \\ 0 \end{pmatrix}.$$

Since the human and the snail populations assume a steady-state value, $\beta_h C\left(\frac{\Lambda_h}{\mu_h+\theta} - S_h\right) \geq 0$ and $\beta_s M\left(\frac{\Lambda_s}{\mu_s+d} - S_s\right) \geq 0$. Hence, it is globally asymptotically stable and this concludes that the infected snails and humans eventually vanish and the disease dies out irrespective of the number of individuals that were initially infected. □

From an epidemiological standpoint, reducing the spread of schistosomiasis is an achievable goal if appropriate control measures are implemented. When transmission rates are reduced, the likelihood of disease resurgence is significantly lower. This not only supports the planning and execution of control efforts but also strengthens strategies aimed at mitigating the spread of the disease by maintaining the reproduction number, R_c, below unity. Furthermore, it provides clear guidance for health workers, who play a crucial role in determining where to concentrate their efforts. Successfully reducing transmission may help shift schistosomiasis elimination from a theoretical concept toward a more tangible objective.

3.5.4. Global stability of the endemic equilibrium state

We investigate the global asymptotic stability of the endemic equilibrium state, E^e, by stating and proving the following theorem.

Theorem 4. *The unique endemic equilibrium E^e, is globally asymptotically stable if $R_c > 1$, and it is not stable if $R_c < 1$.*

Proof. Let $X = (S_h, E_h, M_h, I_h, M, S_s, I_s, C)^T$. Then, we contract a Lyapunov function for the model (9) given as

$$\begin{aligned} V(X) = &\left[S_h - S_h^e - S_h^e \ln\frac{S_h}{S_h^e}\right] + a_1\left[E_h - E_h^e - E_h^e \ln\frac{E_h}{E_h^e}\right] \\ &+ a_2\left[I_h - I_h^e - I_h^e \ln\frac{I_h}{I_h^e}\right] + \left[M_h - M_h^e - M_h^e \ln\frac{M_h}{M_h^e}\right] \\ &+ a_3\left[M - M^e - M^e \ln\frac{M}{M^e}\right] + \left[S_s - S_s^e - S_s^e \ln\frac{S_s}{S_s^e}\right] \\ &+ a_4\left[I_s - I_s^e - I_s^e \ln\frac{I_s}{I_s^e}\right] + a_5\left[C - C^e - C^e \ln\frac{C}{C^e}\right]. \end{aligned} \tag{49}$$

A direct differentiation along the trajectory of the solutions of the model (9) leads to

$$\begin{aligned} V' = &\left[1 - \frac{S_h^e}{S_h}\right]S_h' + a_1\left[1 - \frac{E_h^e}{E_h}\right]E_h' + a_2\left[1 - \frac{I_h^e}{I_h}\right]I_h' \\ &+ \left[1 - \frac{M_h^e}{M_h}\right]M_h' + a_3\left[1 - \frac{M^e}{M}\right]M' \\ &+ \left[1 - \frac{S_s^e}{S_s}\right]S_s' + a_4\left[1 - \frac{I_s^e}{I_s}\right]I_s' + a_5\left[1 - \frac{C^e}{C}\right]C'. \end{aligned} \tag{50}$$

Substituting the system of equations (30) into equation (50) results in

$$\begin{aligned} V' = &\left[1 - \frac{S_h^e}{S_h}\right]\left[\Lambda_h - (1-\omega)\frac{\beta_h C S_h}{1+\varepsilon C} + \eta I_h - \theta S_h - \mu_h S_h\right] \\ &+ a_1\left[1 - \frac{E_h^e}{E_h}\right]\left[(1-\omega)\frac{\beta_h C S_h}{1+\varepsilon C} - k_1 E_h\right] \\ &+ a_2\left[1 - \frac{I_h^e}{I_h}\right][\alpha E_h - k_2 I_h] \\ &+ \left[1 - \frac{M_h^e}{M_h}\right][\theta S_h + \theta E_h + \theta I_h - \mu_h M_h] \\ &+ a_3\left[1 - \frac{M^e}{M}\right][\gamma_h I_h - \mu_m M] \\ &+ \left[1 - \frac{S_s^e}{S_s}\right]\left[\Lambda_s - \frac{\beta_s M S_s}{1+\varepsilon M} - (\mu_s + d)S_s\right] \\ &+ a_4\left[1 - \frac{I_s^e}{I_s}\right]\left[\frac{\beta_s M S_s}{1+\varepsilon M} - k_3 I_s\right] \\ &+ a_5\left[1 - \frac{C^e}{C}\right][\gamma_s I_s - \mu_c C]. \end{aligned} \tag{51}$$

At the endemic equilibrium point, we have the following relations

$$\begin{aligned} &\Lambda_h = (1-\omega)\frac{\beta_h C^e S_h^e}{1+\varepsilon C^e} + \eta I_h^e - \theta S_h^e - \mu_h S_h^e, \\ &k_1 = (1-\omega)\frac{\beta_h C^e S_h^e}{E_h^e(1+\varepsilon C)},\ k_2 = \frac{\alpha E_h^e}{I_h^e},\ \mu_m = \frac{\gamma I_h^e}{M^e}, \\ &\Lambda_s = \frac{\beta M^e S_s^e}{1+\varepsilon M^e} + (\mu_s + d)S_s^e,\ k_3 = \frac{\beta_s M^e S_s^e}{I_s^e(1+\varepsilon M^e)},\ \mu_c = \frac{\gamma_s I_s^e}{C^e}. \end{aligned} \tag{52}$$

Upon substituting equation (51) into equation (52) yields

$$
\begin{aligned}
V' = &\left[1-\frac{S_h^e}{S_h}\right]\left[(1-\omega)\frac{\beta_h(1+\varepsilon C^e)}{C^e S_h^e}\left(1-\frac{CS_h(1+\varepsilon C^e)}{C^e S_h^e(1+\varepsilon C)}\right)\right.\\
&+\eta I_h^e\left(\frac{I_h}{I_h^e}-1\right)+\theta S_h^e\left(1-\frac{S_h}{S_h^e}\right)+\mu_h S_h^e\left(1-\frac{S_h}{S_h^e}\right)]\\
&+a_1\left[1-\frac{E_h^e}{E_h}\right]\left[(1-\omega)\frac{\beta_h(1+\varepsilon C^e}{C^e S_h^e}\left(\frac{CS_h(1+\varepsilon C^e)}{(1+\varepsilon C)C^e S_h^e}-1\right)\right.\\
&\left.+(1-\omega)\frac{\beta_h C^e S_h^e}{1+\varepsilon C^e}\left[1-\frac{E_h^e}{E_h}\right]\right]\\
&+a_2\left[1-\frac{I_h^e}{I_h}\right]\left[\alpha E_h^e\left(\frac{E_h}{E_h^e}-1\right)+\alpha E_h^e\left(1-\frac{I_h}{I_h^e}\right)\right]\\
&+\left[1-\frac{M_h^e}{M_h}\right]\left[\theta\left(\frac{S_h}{S_h^e}-1\right)+\theta\left(\frac{E_h}{E_h^e}-1\right)+\theta\left(\frac{I_h}{I_h^e}-1\right)\right.\\
&\left.+\mu_h M_h^e\left(1-\frac{M_h}{M_h^e}\right)\right]\\
&+a_3\left[1-\frac{M^e}{M}\right]\left[\gamma_h I_h^e\left(\frac{I_h}{I_h^e}-1\right)+\gamma_h I_h^e\left(1-\frac{M}{M^e}\right)\right]\\
&+\left[1-\frac{S_s}{S_s^e}\right]\left[\frac{\beta_s(1+\varepsilon M^e)}{M^e S_s^e}\left(1-\frac{MS_s(1+\varepsilon M^e}{M^e S_s^e(1+\varepsilon M)}\right)\right.\\
&\left.+(\mu_s+d)S_s^e\left(1-\frac{S_s}{S_s^e}\right)\right]\\
&+a_4\left[1-\frac{I_s^e}{I_s}\right]\left[\frac{\beta_s(1+\varepsilon M^e)}{M^e S_s^e}\left(\frac{MS_s(1+\varepsilon M^e}{M^e S_s^e(1+\varepsilon M)}-1\right)\right.\\
&\left.+\frac{\beta_s M^e S_s^e}{1+\varepsilon M^e}\left(1-\frac{I_s}{I_s^e}\right)\right]\\
&+a_5\left[1-\frac{C^e}{C}\right]\left[\gamma_s I_s^e\left(\frac{I_s}{I_s^e}-1\right)+\gamma_s I_s^e\left(1-\frac{C}{C^e}\right)\right].
\end{aligned}
\tag{53}
$$

Let

$$
\begin{aligned}
&\frac{S_h}{S_h^e}=n_1,\ \frac{E_h}{E_h^e}=n_2,\ \frac{I_h}{I_h^e}=n_3,\ \frac{M_h}{M_h^e}=n_4,\ \frac{M}{M^e}=n_5,\\
&\frac{S_s}{S_s^e}=n_6,\ \frac{I_s}{I_s^e}=n_7,\ \frac{C}{C^e}=n_8,\\
&b_1=(1-\omega)\frac{\beta_h(1+\varepsilon C^e)}{C^e S_h^e},\ b_2=\frac{1+\varepsilon C^e}{1+\varepsilon C},\\
&b_3=\eta I_h^e,\ b_4=\theta S_h^e,\ b_5=\alpha E_h^e,\ b_6=\gamma_h I_h^e,\\
&b_7=\frac{\beta_s(1+\varepsilon M^e)}{M^e S_s^e},\ b_8=\frac{1+\varepsilon M^e}{1+\varepsilon M},\\
&b_9=\gamma_s I_s^e,\ b_{10}=(1-\omega)\frac{\beta_h C^e S_h^e}{1+\varepsilon C^e},\\
&b_{11}=\frac{\beta_s M^e S_s^e}{1+\varepsilon M^e}, b_{12}=\theta E_h^e,\ b_{13}=\theta I_h^e.
\end{aligned}
\tag{54}
$$

Then,

$$
\begin{aligned}
V' = &-\left[\mu_h S_h^e\frac{(1-n_1)^2}{n_1}+\mu_h^e\frac{(1-n_4)^2}{n_4}+(\mu_s+d)S_s^e\frac{(1-n_6)^2}{n_6}\right]\\
&+\left[1-\frac{1}{n_1}\right](b_1-b_1b_2n_1n_8+b_3n_3-b_3+b_4-b_4n_1)\\
&+a_1\left[1-\frac{1}{n_2}\right](b_1b_2n_1n_8-b_1+b_{10}-b_{10}n_2)\\
&+a_2\left[1-\frac{1}{n_3}\right](b_5n_2-b_5+b_5-b_5n_3)\\
&+\left[1-\frac{1}{n_4}\right](b_4n_1-b_4+b_{12}n_2-b_{12}+b_{13}n_3-b_{13})\\
&+a_3\left[1-\frac{1}{n_5}\right](b_6n_3-b_6+b_6-b_6n_5)\\
&+\left[1-\frac{1}{n_6}\right](b_7-b_7b_8n_5n_6)\\
&+a_4\left[1-\frac{1}{n_7}\right](b_7b_8n_5n_6-b_7+b_{11}-b_{11}n_7)\\
&+a_5\left[1-\frac{1}{n_8}\right](b_9n_7-b_9+b_9-b_9n_8).
\end{aligned}
\tag{55}
$$

The $b_i s,\ i\in[1,13]$ are carefully selected such that $a_1=a_4=1$, $a_2=a_3=0$ and $a_5=\frac{b_{11}}{b_9}$. Thus, equation (55) becomes

$$
\begin{aligned}
V' = &-\left[\mu_h S_h^e\frac{(1-n_1)^2}{n_1}+\mu_h M_h^e\frac{(1-n_4)^2}{n_4}+(\mu_s+d)S_s^e\frac{(1-n_6)^2}{n_6}\right]\\
&+b_3\left(n_3-1+\frac{1}{n_1}-\frac{n_3}{n_1}\right)+b_4\left(1-\frac{n_1}{n_4}+\frac{1}{n_4}-\frac{1}{n_1}\right)\\
&+b_{10}\left(2-n_2-\frac{1}{n_2}\right)+b_{11}\left(1-\frac{1}{n_7}-n_8-\frac{n_7}{n_8}\right)\\
&+b_{12}\left(n_2-1-\frac{n_2}{n_4}+\frac{1}{n_4}\right)+b_{13}\left(n_3-1-\frac{n_3}{n_4}+\frac{1}{n_4}\right).
\end{aligned}
\tag{56}
$$

Let us examine the function $v(x)=1-x+\ln(x)$, which satisfies $v(x)\le 0$ for all $x>0$, with equality occurring precisely at $x=1$. Given that $1-x\le-\ln(x)$, it follows that the b_3 term transforms into

$$
(1-\tfrac{n_3}{n_1})-(1-n_3)-(1-\tfrac{1}{n_1})\le-\ln\tfrac{n_3}{n_1}+\ln n_3+\ln\tfrac{1}{n_1}=\ln(\tfrac{n_1}{n_3}\cdot n_3\cdot\tfrac{1}{n_1})=0.
$$

Similarly, the $b_4,\ b_{11}, b_{12}$ and b_{13} terms become

$$
\left(1-\frac{n_1}{n_4}\right)-\left(1-\frac{1}{n_4}\right)+\left(1-\frac{1}{n_1}\right)\le-\ln\frac{n_1}{n_4}+\ln\frac{1}{n_4}-\ln\frac{1}{n_1}=\ln\left(\frac{n_4}{n_1}\cdot\frac{1}{n_4}\cdot n_1\right)=0,
$$

$$
\left(1-\frac{1}{n_7}\right)+(1-n_8)-\left(1+\frac{n_7}{n_8}\right)\le-\ln\frac{1}{n_7}-\ln n_8-\ln\frac{n_7}{n_8}=\ln\left(n_7\cdot\frac{1}{n_8}\cdot\frac{n_8}{n_7}\right)=0,
$$

$$
\left(1-\frac{n_2}{n_4}\right)-(1-n_2)-\left(1-\frac{1}{n_4}\right)\le-\ln\frac{n_2}{n_4}+\ln n_2+\ln\frac{1}{n_4}=\ln\left(\frac{n_4}{n_2}\cdot n_2\cdot\frac{1}{n_4}\right)=0,
$$

$$
\left(1-\frac{n_3}{n_4}\right)-(1-n_3)-\left(1-\frac{1}{n_4}\right)\le-\ln\frac{n_3}{n_4}+\ln n_3+\ln\frac{1}{n_4}=\ln\left(\frac{n_4}{n_3}\cdot n_3\cdot\frac{1}{n_4}\right)=0.
$$

Applying the Arithmetic mean-Geometric mean inequality on the b_{10} term results in

$$
V'=-\left[\mu_h S_h^e\frac{(1-n_1)^2}{n_1}+\mu_h M_h^e\frac{(1-n_4)^2}{n_4}+(\mu_s+d)S_s^e\frac{(1-n_6)^2}{n_6}\right]\le 0.
$$

By LaSalle's invariance principle [40], we can conclude that as $t \longrightarrow \infty$, for $R_c > 1$, the endemic equilibrium state, E_e, is globally asymptotically stable. □

This implies that, in areas where schistosomiasis is endemic, the disease continues to spread between humans and snails, thereby maintaining a consistent level of prevalence. Consequently, short-term or small-scale interventions are insufficient to address the problem. Comprehensive intervention strategies are required, including regular mass drug administration (represented by θ), snail control programmes (represented by d), and public enlightenment campaigns (represented by ω).

As the disease reaches a steady state, where the number of new infections equals the number of recoveries and deaths, health officials can use this information to plan and allocate resources more effectively. Schistosomiasis will persist within the population unless significant changes are made to its transmission dynamics, emphasising the need for a coordinated and comprehensive approach to disease control.

4. Numerical simulations

Schistosomiasis continues to be classified as a neglected tropical disease with significant public health implications, particularly across Africa. In Nigeria, it remains highly prevalent [1, 2]. Consequently, when conducting numerical simulations of the disease, it is essential to calibrate model parameters to reflect real-world situations. This ensures the simulation's accuracy and relevance to Nigeria's specific context.

4.1. Parameter estimation

In this study, we examined a case where the human population remains steady at 1 million people. We used the average life expectancy in Nigeria to estimate the natural death rate, which comes out to about $\mu_h = \frac{1}{54\times365} = 5.0735 \times 10^{-5}$ per day [41]. We estimate that about $\Lambda_h = 1000000 \times \mu_h$ recruited persons are added to the population each day, with the assumption that a year has 365 days. A study in Sudan by Kheir *et al.* [30] found that out of every 1,000 people infected with *Schistosoma mansoni*, one person dies each year. Based on this, we set the daily death rate from the disease as $\delta_h = 0.0000027$. We assumed that people recover on their own in about 6 weeks, which corresponds to a recovery rate of $\eta = \frac{1}{43} = 0.02325$ per day.

The miracidia stage of *S. mansoni* lasts for a short time, typically 5, 6, or 9 hours [42]. Based on this, we set the death rate at about $\mu_m = \frac{20}{3\times24} = 0.2778$ per day. Similarly, the cercariae stage of *S. mansoni* lasts approximately 10.5 hours on average (ranging from 8 to 17 hours) [43]. So, we set the death rate as $\mu_c = \frac{10.5}{24} = 0.4375$ per day. According to estimates from McCreesh *et al.* [28], infected humans release the parasite at a rate of 0.00232 per day, whereas infected snails release it approximately 2.6 times per day. These values indicate the frequency at which the infectious stages of schistosomiasis enter the environment. Also, the growth velocity of the pathogen, ε is limited by a rate of 0.2 [10].

We assumed the recruitment rate for the snail population is 20000 per day and used an average snail death rate of about 12 deaths every 6.5 years, which works out to roughly 1.85 deaths per year, or 5.0685×10^{-3} per day. Due to infection, snails die at a rate of $\delta_s = 4.012 \times 10^{-4}$ per day, based on findings from McCreesh *et al.* [28].

4.1.1. Baseline plots

Using the parameter values in Table 1, we performed numerical simulations of the system of equations (9) with initial conditions given as $(S_h, E_h, I_h, M_h, M, S_s, I_s, C) = (10000, 0, 0, 0, 1, 8000, 0, 1)$.

Figure 3 shows how the system behaves when there is no public enlightenment campaign (ω), no snail control measure (d), and no mass drug administration (θ). From the plot, we can see that the number of exposed humans (E_h) and infected humans (I_h) increases very quickly. At the same time, the number of people who are still susceptible and those in the drug administration compartment drops to almost zero (see Figure 3a). Similarly, Figure 3b shows that the infected snail population (I_s) grows rapidly, while the population of healthy, susceptible snails (S_s) gradually disappears. Additionally, the cercaria and the miracidia populations also increase with time.

In Figure 4, we analyse the dynamics of the system of equations (9) at $\omega = 0.2$ with $\theta = d = 0$. It is evident that the number of infected individuals continues to rise, even with a public enlightenment rate of 20%. This unexpected outcome indicates that merely raising awareness is insufficient to control the spread of schistosomiasis. Without complementary changes in attitudes or the implementation of interventions such as mass drug administration or environmental modifications to control snail populations, information alone does not lead to effective disease management.

In Figure 5, where $\theta = 0.2$ and both ω and d are equal to 0, the M_h compartment shows a sporadic increase. In contrast, the compartments for miracidia and cercariae peak at relatively lower values. Although the I_s compartment continues to grow, it reaches its peak more quickly and with fewer infected snails compared with scenarios without mass drug administration. This outcome results from the effects of drug usage, which decreases the worm burden in the human population. Consequently, this reduction influences the rate at which infected individuals shed parasites into the environment.

Figure 6 illustrates the dynamics of the system described by the equations in (9) under the conditions $d = 0.2$, $\omega = 0$, and $\theta = 0$. With these parameters, the E_h compartment shows sporadic growth, although at a slower rate compared to situations without snail control measures. Additionally, the miracidia compartment exhibits irregular growth patterns, whereas the cercaria compartment reaches its peak more quickly, albeit at a lower overall value. This behaviour can be attributed to the decreased snail population in the environment, which directly leads to a reduction in the number of cercariae released. Consequently, the overall transmission potential of the parasite is diminished.

In Figure 7, the M_h compartment shows sporadic growth, while the compartments for miracidia (M), cercariae (C), and

infected snails (I_s) all peak at lower values.

This outcome is due to the control parameters being set at $\omega = \theta = d = 0.2$, which significantly impact the system's dynamics. These parameters represent strategic interventions such as drug administration, snail control, and public enlightenment campaigns. Implementing such measures could help mitigate the spread of schistosomiasis by reducing the populations responsible for disease transmission and infection.

4.2. Sensitivity analysis

To identify the key parameters for intervention strategies aimed at reducing the spread of schistosomiasis, it is crucial to understand how these parameters influence the disease dynamics. This requires conducting a sensitivity analysis on the control reproduction number, to assess how variations in different parameters affect it. The analysis will employ the normalised forward sensitivity indices, defined as follows:

$$\Gamma_A^{R_c} = \frac{\partial R_c}{A} \times \frac{A}{R_c}, \tag{57}$$

where A is any parameter of R_c [44]. The sensitivity indices of the parameters of the control reproduction number, R_c, are shown in Figure 8.

The sign of the sensitivity indices (whether positive or negative) indicates how input variables influence the outcome. A positive index implies that, as the input variable increases, the number of future schistosomiasis cases will also rise. Conversely, a negative index signifies that an increase in the input variable will lead to a reduction in future cases of schistosomiasis.

Specifically, the public enlightenment rate (ω), the disease-induced death rate for the snail population (δ_s), environmental modifications for snail control (d), the mortality rates for the cercaria and miracidia populations (μ_c and μ_m), the recovery rate for the human population (η), the progression rate into the MDA class (θ), and the mortality rate for the snail population (μ_s) all exhibit an inverse relationship with the control reproduction number (R_c).

This means that increases in any of the variables ω, δ_s, d, $\mu_c, \mu_m, \eta, \theta$, or μ_s lead to a decrease in the transmission potential of schistosomiasis. For instance, a 1% increase in μ_c, μ_m, or η results in approximately a 0.88% reduction in R_c, while a 1% increase in θ reduces R_c by roughly 0.7%. A 1% rise in μ_s lowers R_c by about 0.8%, all demonstrating a strong negative sensitivity.

In contrast, an increase in α, γ_h, γ_s, β_h, β_s, or Λ_s will result in a rise in future schistosomiasis cases, as these factors directly influence the rate at which the disease spreads. For example, if $\gamma_s, \gamma_h, \beta_h, \beta_s$, or Λ_s each increase by 1%, the basic reproduction number R_c will increase by approximately 0.5%, indicating a strong positive influence on disease transmission dynamics.

We employed the Latin Hypercube Sampling–Partial Rank Correlation Coefficient (LHS–PRCC) method on the schistosomiasis model (9) to examine how different parameters influence the various infected classes within the system. This analysis provides a comprehensive understanding of the parameter space in relation to different population variables, as illustrated in Figure 9. We assumed that the parameters are uniformly distributed, and considered various response functions, including E_h, I_h, M, I_s, and C, to conduct our analysis.

The effectiveness of this approach is evaluated by calculating the PRCC values, which reveal the sensitivity of the parameters within the schistosomiasis model. To obtain these values, the LHS method was employed to stratify the samples without replacement. Baseline values for the parameters were first established, followed by simulations to perform the PRCC analysis. The magnitude and direction of the PRCC values for the distinct parameters are crucial in understanding each parameter's contribution to the model's predictive accuracy.

PRCC values greater than 0.5 or less than -0.5 are particularly significant [45], as they indicate a substantial impact on the outcomes measured by the LHS parameters. Figure 9(f) supports the findings presented in Figure 8, demonstrating the influence of each parameter on the control reproduction number, R_c. This suggests a higher level of uncertainty in the fluctuation of infected cases.

Overall, we observe that the correlations between each variable and its corresponding parameter, as indicated by the PRCC values, are consistent with the behaviour predicted by the respective model equations.

4.3. Simulation results

By using the parameter values in Table 1, we investigate the performance of sensitive parameters in the infected compartments.

Figure 10 illustrates that increases in the effective contact rate between humans and cercariae and in the shedding rate for the infected human class (β_h and γ_h) results in a higher number of individuals falling into the Exposed and Infected categories, as depicted in Figures 10a and 10d. This rise in infection rates also leads to an increase in the number of miracidia, the parasite stage that originates from human waste, as shown in Figure 10c. Notably, this occurs despite public enlightenment campaign efforts (ω), the progression into treatment programmes (θ), and snail control measures (d) all remaining at 50%.

This highlights the essential role of public enlightenment campaigns in promoting proper waste disposal. These campaigns should not only focus on educating the public but also actively advocate for the safe disposal of faeces, for example through the construction of adequate toilet facilities. Such a proactive approach is crucial in preventing miracidia from reaching freshwater environments, where they can infect snails and perpetuate transmission. Furthermore, the campaigns should emphasise the benefits of mass drug administration (MDA), which reduces the worm burden in exposed and infected individuals, thereby slowing the spread of the disease.

In Figure 11, when public enlightenment campaigns (ω), snail control (d), and treatment progression (θ) are maintained at 50%, we still observe an increase in both the number of infected snails, as shown in Figure 11d, and the cercaria population, displayed in Figure 11e. This indicates that enlightenment campaigns alone are insufficient to halt the spread of infection.

Therefore, public enlightenment campaigns should promote actions aimed at reducing the snail population in the environment, such as treating water bodies or introducing natural predators of snails, including the pea puffer fish.

5. Conclusion

We investigated the transmission of schistosomiasis between humans and snails. In this disease, cercariae infect humans, while miracidia infect snails. Using a mathematical model, we incorporated essential factors such as mass drug administration (MDA), public enlightenment campaigns, and environmental modifications to control snail populations. We calculated the control reproduction number, R_c, which provides insight into how easily the disease can spread. The results indicated that increasing participation in MDA programmes (θ) and raising snail mortality rates (d) are the most effective strategies for reducing the reproduction number, R_c, and consequently lowering the transmission rate. Additionally, we examined the stability of the system over time. We found that enhancing public enlightenment, improving environmental control of snails, and encouraging participation in MDA programmes can help prevent the spread of the disease. We also investigated how contact rates between healthy humans and cercariae, as well as between healthy snails and miracidia, influence the transmission of schistosomiasis, while keeping public enlightenment, MDA participation, and snail control efforts constant at 50%.

The results suggest that enlightenment campaigns should not only inform the public but also promote practical actions, such as the proper use of toilet facilities to prevent contamination of water bodies, participation in MDA programmes to reduce parasite levels in humans, and strategies to lower snail populations, including the introduction of snail-eating predators. This approach is crucial because enlightenment alone is insufficient; campaigns must translate into actual behavioural change.

This study has some limitations. We relied on data from previous research and had to make certain assumptions, such as the manner in which snails are recruited into the population. Moreover, we did not account for seasonal variations, even though changes in season can influence attitudes and behaviours in both humans and snails. Nonetheless, our findings align with the observations of King and Bertsch [26], who suggested that mass drug administration (MDA) programmes can effectively reduce the incidence of schistosomiasis as well as its transmission. These insights can assist policymakers in developing more effective strategies to combat schistosomiasis and mitigate its impact.

Data availability

No additional data were used beyond those presented in the submitted manuscript.

Acknowledgment

This work was partially supported by a grant from the IMU-CDC under the IMU-CDC GRAID Program.

References

[1] E. Bottieau, M. Mbow, I. Brosius, C. Roucher, C. T. Gueye, O. T. Mbodj, B. T. Faye, A. De Hondt, B. Smekens, D. Arango, C. Burm, A. Tsoumanis, L. Paredis, Y. Van Herrewege, I. Potters, J. Richter, A. Rosanas-Urgell, B. Cisse, S. Mboup & K. Polman, "Antimalarial artesunate–mefloquine versus praziquantel in African children with schistosomiasis: an open-label, randomized controlled trial", Nature Medicine **30** (2024) 130. https://doi.org/10.1038/s41591-023-02719-4.

[2] I. Bada, I. I. Ako, R. U. Akhaze & O. O. Olowu, "Mathematical analysis of schistosomiasis with case detection", Journal of the Nigerian Association of Mathematical Physics **59** (2021) 1. https://www.researchgate.net/publication/371811583_MATHEMATICAL_ANALYSIS_OF_SCHISTOSOMIASIS_WITH_CASE_DETECTION.

[3] A. Idan & H. A. M. Al-Saady, "Schistosomiasis in Iraq: a mini-review of literature", The Medical Journal of Basrah University **42** (2024) 28. https://doi.org/10.33762/mjbu.2024.145555.1181.

[4] World Health Organization, *Schistosomiasis*. [Online]. https://www.who.int/news-room/fact-sheets/detail/schistosomiasis. [Accessed: Sep. 28, 2024].

[5] P. A. Mawa, J. Kincaid-Smith, E. M. Tukahebwa, J. P. Webster & S. Wilson, "Schistosomiasis morbidity hotspots: roles of the human host, the parasite and their interface in the development of severe morbidity", Frontiers in Immunology **12** (2021) 635869. https://doi.org/10.3389/fimmu.2021.635869.

[6] Y. Qi, M. Huang, H. Sun, X. Wu, Z. Liu & D. Lu, "Prevalence of depressive symptoms in patients with advanced schistosomiasis in China", PLoS Neglected Tropical Diseases **18** (2024) e0012003. https://doi.org/10.1371/journal.pntd.0012003.

[7] P. Ogongo, R. K. Nyakundi, G. K. Chege & L. Ochola, "The road to elimination: current state of schistosomiasis research and progress towards the end game", Frontiers in Immunology **13** (2022) 846108. https://doi.org/10.3389/fimmu.2022.846108.

[8] D. Gurarie & C. H. King, "Population biology of *Schistosoma* mating, aggregation, and transmission breakpoints: more reliable model analysis for the end-game in communities at risk", PLoS ONE **9** (2014) e115875. https://doi.org/10.1371/journal.pone.0115875.

[9] M. T. Inobaya, R. M. Olveda, T. N. P. Chau, D. U. Olveda & A. G. P. Ross, "Prevention and control of schistosomiasis: a current perspective", Research and Reports in Tropical Medicine **5** (2015) 65. https://doi.org/10.2147/RRTM.S44274.

[10] T. Chiyaka & W. Garira, "Mathematical analysis of the transmission dynamics of schistosomiasis in the human-snail hosts", Journal of Biological Systems **17** (2009) 397. https://doi.org/10.1142/S0218339009002910.

[11] S. Kadaleka, S. Abelman, P. M. Mwamtobe & J. M. Tchuenche, "Optimal control analysis of a human-bovine schistosomiasis model", Journal of Biological Systems **29** (2021) 1. https://doi.org/10.1142/S0218339021500017.

[12] E. Kanyi, A. S. Afolabi & N. O. Onyango, "Mathematical modelling and analysis of transmission dynamics and control of schistosomiasis", Journal of Applied Mathematics **2021** (2021) 6653796. https://doi.org/10.1155/2021/6653796.

[13] O. Koutou, B. Traore & B. Sangare, "Analysis of schistosomiasis global dynamics with general incidence functions and two delays", International Journal of Applied and Computational Mathematics **7** (2021) 1. https://doi.org/10.1007/s40819-021-01188-y.

[14] S. Lopez, S. Majid, R. Syed, J. Rychtar & D. Taylor, "Mathematical model of voluntary vaccination against schistosomiasis", PeerJ **12** (2024) e16869. https://doi.org/10.7717/peerj.16869.

[15] W. Nur, S. Trisilowati, A. Suryanto & W. M. Kusumawinahyu, "Mathematical modelling of schistosomiasis transmission dynamics in traditional cattle farmer communities", Advances in Social Science, Education and Humanities Research **550** (2020) 123. https://doi.org/10.2991/assehr.k.210508.105.

[16] W. Nur, S. Trisilowati, A. Suryanto & W. M. Kusumawinahyu, "Model incorporating snail predator as biological control agent", Mathematics **9** (2021) 1858. https://doi.org/10.3390/math9161858.

[17] M. Ronoh, F. Chirove, S. A. Pedro, M. S. S. Tchamga, C. E. Madubueze, S. C. Madubueze, J. Addawe, P. M. Mwamtobe & K. R. Mbra, "Modelling the spread of schistosomiasis in humans with environmental transmission", Applied Mathematical Modelling **95** (2021) 1. https://doi.org/10.1016/j.apm.2021.01.046.

[18] Z. Tabo, C. Kalinda, L. Breuer & C. Albrecht, "Adapting strategies for effective schistosomiasis prevention", Mathematics **11** (2023) 2609. https://doi.org/10.3390/math11122609.

[19] A. Abokwara & C. E. Madubueze, "The role of non-pharmacological interventions on the dynamics of schistosomiasis", Journal of Mathematical and Fundamental Sciences **53** (2021) 243. https://doi.org/10.5614/j.math.fund.sci.2021.53.2.6.

[20] E. Madubueze, R. I. Gweryina & A. Abokwara, "Mathematical analysis and optimal control of schistosomiasis transmission model", Biomath Communications **9** (2022) 071. https://doi.org/10.11145/bmc.2022.03.071.

[21] D. Temfack, "Mathematical modelling of schistosomiasis transmission using reaction-diffusion equations", Fundamental Journal of Mathematics and Applications **7** (2024) 45. https://doi.org/10.33401/fujma.1412958.

[22] P. Wu, Y. Salmaniw & X. Wang, "Threshold dynamics of a reaction–advection–diffusion schistosomiasis epidemic model", Journal of Mathematical Biology **88** (2024) 1. https://doi.org/10.1007/s00285-024-02097-6.

[23] Z. Tabo, L. Luboobi, P. Kraft & C. Albrecht, "Control of schistosomiasis by intermediate hosts", Mathematical Biosciences **376** (2024) 109263. https://doi.org/10.1016/j.mbs.2024.109263.

[24] H. C. Turner, J. E. Truscott, A. A. Bettis, S. H. Farrell, A. K. Deol, J. M. Whitton, F. M. Fleming, & R. M. Anderson, "Evaluating the variation in the projected benefit of community-wide mass treatment for schistosomiasis: implications for future economic evaluations", Parasites & Vectors **10** (2017) 213. https://doi.org/10.1186/s13071-017-2141-5.

[25] World Health Organization, *Field use of molluscicides in schistosomiasis control programmes: An operational manual for programme managers*, World Health Organization, Geneva, Switzerland, 2017. ISBN: 978-92-4-151199-5.

[26] H. King & D. Bertsch, "Historical perspective: Snail control to prevent schistosomiasis", PLoS Neglected Tropical Diseases **9** (2015) e0003657. https://doi.org/10.1371/journal.pntd.0003657.

[27] E. Madubueze, Z. Chazuka, I. O. Onwubuya, F. Fatimawati & C. W. Chukwu, "On the mathematical modelling of schistosomiasis transmission dynamics with heterogeneous intermediate host", Frontiers in Applied Mathematics and Statistics **8** (2022) 1020161. https://doi.org/10.3389/fams.2022.1020161.

[28] N. McCreesh, G. Nikulin & M. Booth, "Predicting the effects of climate change on Schistosoma mansoni transmission in eastern Africa", Parasites & Vectors **8** (2015) 4. https://doi.org/10.1186/s13071-014-0617-0.

[29] C. Appleton, "The influence of temperature on the life-cycle and distribution of Biomphalaria pfeifferi (Krauss, 1948) in south-eastern Africa", International Journal for Parasitology **7** (1977) 335. https://doi.org/10.1016/0020-7519(77)90057-1.

[30] M. Kheir, I. A. Eltoum, A. M. Saad, M. M. Ali, O. Z. Baraka & M. Homeida, "Mortality due to Schistosoma mansoni: A field study in Sudan", The American Journal of Tropical Medicine and Hygiene **60** (1999) 307. https://doi.org/10.4269/ajtmh.1999.60.307.

[31] G. Birkhoff & C. Rota, *Ordinary Differential Equations*, 4th ed., John Wiley & Sons, Hoboken, NJ, USA, 1998. ISBN: 9780471860037.

[32] P. Van den Driessche & J. Watmough, "Reproduction numbers and subthreshold endemic equilibria", Mathematical Biosciences **180** (2002) 29. https://doi.org/10.1016/S0025-5564(02)00108-6.

[33] M. Heffernan, R. J. Smith & L. M. Wahl, "Perspectives on the basic reproductive ratio", Journal of the Royal Society Interface **2** (2005) 281. https://doi.org/10.1098/rsif.2005.0042.

[34] A. Abokwara & C. E. Madubueze, "Optimizing the control of lymphatic filariasis: A mathematical modelling and cost-effectiveness analysis", Discover Public Health **22** (2025) 703. https://doi.org/10.1186/s12982-025-01058-8.

[35] C. Castillo-Chavez & B. Song, "Dynamical models of tuberculosis and their applications", Mathematical Biosciences and Engineering **1** (2004) 361. https://doi.org/10.3934/mbe.2004.1.361.

[36] World Health Organization, *Ending the Neglect to Attain the Sustainable Development Goals: A Road Map for Neglected Tropical Diseases 2021–2030*, World Health Organization, Geneva, Switzerland, 2021. https://www.who.int/publications/i/item/9789240010352.

[37] G. Colley, A. L. Bustinduy, W. E. Secor & C. H. King, "Human schistosomiasis", The Lancet **383** (2014) 2253. https://doi.org/10.1016/S0140-6736(13)61949-2.

[38] H. King, "Parasites and poverty: The case of schistosomiasis", Acta Tropica **113** (2010) 95. https://doi.org/10.1016/j.actatropica.2009.11.012.

[39] C. Castillo-Chavez, Z. Feng & W. Huang, "On the computation of R_0 and its role on global stability", in *Mathematical Approaches for Emerging and Reemerging Infectious Diseases*, Springer, New York, USA, 2002, pp. 229–250. https://www.researchgate.net/publication/228915276.

[40] J. LaSalle & S. Lefschetz, *The Stability of Dynamical Systems*, SIAM, Philadelphia, PA, USA, 1976. ISBN: 9780898710158.

[41] World Development Indicators, *Life expectancy at birth, total (years) – Nigeria*. [Online]. https://data.worldbank.org/indicator/SP.DYN.LE00.IN?locations=NG. [Accessed: Jun. 20, 2025].

[42] F. Maldonado & J. Acosta-Matienzo, "Biological studies on the miracidium of Schistosoma mansoni", American Journal of Tropical Medicine **28** (1948) 645. https://doi.org/10.4269/ajtmh.1948.s1-28.645.

[43] P. Whitfield, A. Bartlett, N. Khammo & R. Clothier, "Age-dependent survival and infectivity of Schistosoma mansoni cercariae", Parasitology **127** (2003) 29. https://doi.org/10.1017/S0031182003003263.

[44] N. Marsudi, Hidayat & R. B. E. Wibowo, "Optimal control and sensitivity analysis of HIV model with public health education campaign and antiretroviral therapy", AIP Conference Proceedings **2021** (2018) 060033. https://doi.org/10.1063/1.5062797.

[45] R. Bandekar & M. Ghosh, "A coinfection model on TB–COVID-19 with optimal control and sensitivity analysis", Mathematics and Computers in Simulation **200** (2022) 1. https://doi.org/10.1016/j.matcom.2022.04.001.